Nuclear matrix elements for double-β decay

J. Barea, J. Kotila, and F. Iachello

Phys. Rev. C **87**, 014315 — Published 14 January 2013

DOI: 10.1103/PhysRevC.87.014315

Nuclear matrix elements for double-β decay

J. Barea,[1,*] J. Kotila,[2,†] and F. Iachello[2,‡]

[1] *Departamento de Física, Universidad de Concepción, Casilla 160-C, Concepción, Chile*
[2] *Center for Theoretical Physics, Sloane Physics Laboratory, Yale University, New Haven, CT 06520-8120, USA*

Background: Direct determination of the neutrino mass through double-β decay is at the present time one of the most important areas of experimental and theoretical research in nuclear and particle physics. Purpose: Calculate nuclear matrix elements for the extraction of the average neutrino mass in neutrinoless double-β decay. Methods: The microscopic interacting boson model (IBM-2) is used. Results: Nuclear matrix elements in the closure approximation are calculated for ^{48}Ca, ^{76}Ge, ^{82}Se, ^{96}Zr, ^{100}Mo, ^{110}Pd, ^{116}Cd, ^{124}Sn, ^{128}Te, ^{130}Te, ^{148}Nd, ^{150}Nd, ^{154}Sm, ^{160}Gd, and ^{198}Pt decay. Conclusions: Realistic predictions for the expected half-lives in neutrinoless double-β decay with light and heavy neutrino exchange in terms of neutrino masses are made and limits are set from current experiments.

PACS numbers: 23.40.Hc,21.60.Fw,27.50.+e,27.60.+j

I. INTRODUCTION

In recent years, the possibility of a direct measurement of the average neutrino mass in neutrinoless double-β decay has attracted considerable attention. Three scenarios have been considered [1–3], shown in Fig. 1. After the discovery of neutrino oscillations [4–6], attention has been focused on the first scenario (a). In very recent years, the second scenario (b) has attracted again attention [7]. For all three processes ($0\nu\beta\beta$, $0\nu_h\beta\beta$, $0\nu\beta\beta M$), the half-life can be factorized as

$$[\tau^{0\nu}_{1/2}]^{-1} = G_{0\nu} \left|M_{0\nu}\right|^2 \left|f(m_i, U_{ei})\right|^2 , \qquad (1)$$

where $G_{0\nu}$ is a phase space factor, $M_{0\nu}$ the nuclear matrix element and $f(m_i, U_{ei})$ contains physics beyond the standard model through the masses m_i and mixing matrix elements U_{ei} of neutrino species.

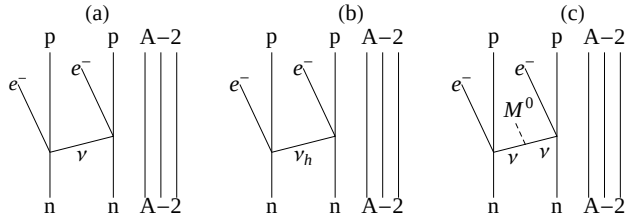

Figure 1. Neutrinoless double-β decay mechanism for (a) light neutrino exchange, (b) heavy neutrino exchange and (c) Majoron emission.

In addition to the neutrinoless modes, there is also the process allowed by the standard model, $2\nu\beta\beta$, depicted in Fig. 2. For this process, the half-life can be, to a good approximation, factorized in the form

$$\left[\tau^{2\nu}_{1/2}\right]^{-1} = G_{2\nu} \left|M_{2\nu}\right|^2 . \qquad (2)$$

[The factorization here is not exact and conditions under which it can be done are discussed in Ref. [8] and Sect. III].

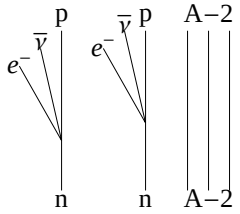

Figure 2. Double-β decay mechanism with the emission of $2\bar{\nu}$.

The processes depicted in Figs. 1 and 2 are of the type

$$(A, Z) \rightarrow (A, Z+2) + 2e^- + \text{anything}. \qquad (3)$$

In very recent years, interest in the processes

$$(A, Z) \rightarrow (A, Z-2) + 2e^+ + \text{anything} \qquad (4)$$

has also arisen. In this case there are also the competing modes in which either one or two electrons are captured from the electron cloud ($0\nu\beta$EC, $2\nu\beta$EC, 2νECEC). Also for these modes, the half-life can be factorized (either exactly or approximately) into the product of a phase space factor and a nuclear matrix element which then are the crucial ingredients of any double-β decay calculation.

Recently, we have initiated a program for the systematic evaluation of both quantities. The evaluation of the phase space factors (PSF) for $0\nu\beta^-\beta^-$ and $2\nu\beta^-\beta^-$ has been reported in [8] and that for $0\nu\beta^+\beta^+$, $2\nu\beta^+\beta^+$, $0\nu\beta^+$EC, $2\nu\beta^+$EC, 2νECEC, is in preparation [9]. The main difference of this new calculation of PSFs as compared with older standard approximations is few percent

* jbarea@udec.cl
† jenni.kotila@yale.edu
‡ francesco.iachello@yale.edu

for light nuclei ($Z = 20$), about 30% for Nd ($Z = 60$) and a rather large 90% for U ($Z = 92$), the correction increasing as a power of $Z\alpha$. In this article, we concentrate on nuclear matrix elements, $M_{0\nu}$, $M_{2\nu}$, for $0\nu\beta^-\beta^-$ and $2\nu\beta^-\beta^-$. Calculations of the nuclear matrix elements for positron emission have also been completed and will be reported in a subsequent paper [10]. Nuclear matrix elements have been evaluated in a variety of models, most notably the quasi-particle random phase approximation (QRPA) and the shell model (ISM). Results up to 1998 are reviewed in Refs. [11] and [12]. In 1999 a new formulation of $0\nu\beta\beta$ was introduced [3] and calculations within the QRPA [13] and ISM [14] were performed, as well as in other models, as discussed in the following Sect. II. C. In 2009, we developed [15] a new method to evaluate nuclear matrix elements for double-β decay within the framework of the microscopic interacting boson model (IBM-2). The advantage of this method is that it can be used in any nucleus and thus all nuclei of interest both in $\beta^-\beta^-$ and $\beta^+\beta^+$ decay can be calculated within the same model.

The calculation of the nuclear matrix elements is done in the *closure* approximation. This approximation is good for $0\nu\beta\beta$ decay, since the average neutrino momentum is of the order of 100 MeV/c. It is, in principle, not good for $2\nu\beta\beta$, since the average neutrino momentum is of the order of few MeV/c. However, formally the approximation is still valid if one appropriately defines the closure energy. The advantage of the closure approximation is that all calculations for the processes depicted in Figs. 1 and 2 can be done simultaneously, by changing the so-called neutrino "potential", as discussed in the sections below, thus eliminating systematic (and accidental) errors in the calculation, especially in the ratio of matrix elements for different processes.

Table I. Double-β decays considered in this article, their Q-values and their isotopic abundances.

$\beta^-\beta^-$ transition	$Q_{\beta\beta}$(keV)	P(%)
$^{48}_{20}Ca_{28} \rightarrow ^{48}_{22}Ti_{26}$	4272.26 ± 4.04	0.187 ± 0.021
$^{76}_{32}Ge_{44} \rightarrow ^{76}_{34}Se_{42}$	2039.061 ± 0.007	7.73 ± 0.12
$^{82}_{34}Se_{48} \rightarrow ^{82}_{36}Kr_{46}$	2995.12 ± 2.01	8.73 ± 0.22
$^{96}_{40}Zr_{56} \rightarrow ^{96}_{42}Mo_{54}$	3350.37 ± 2.89	2.80 ± 0.09
$^{100}_{42}Mo_{58} \rightarrow ^{100}_{44}Ru_{56}$	3034.40 ± 0.17	9.82 ± 0.31
$^{110}_{46}Pd_{64} \rightarrow ^{110}_{48}Cd_{62}$	2017.85 ± 0.64	11.72 ± 0.09
$^{116}_{48}Cd_{68} \rightarrow ^{116}_{50}Sn_{66}$	2813.50 ± 0.13	7.49 ± 0.18
$^{124}_{50}Sn_{74} \rightarrow ^{124}_{52}Te_{72}$	2286.97 ± 1.53	5.79 ± 0.05
$^{128}_{52}Te_{76} \rightarrow ^{128}_{54}Xe_{74}$	865.87 ± 1.31	31.74 ± 0.08
$^{130}_{52}Te_{78} \rightarrow ^{130}_{54}Xe_{76}$	2526.97 ± 0.23	34.08 ± 0.62
$^{136}_{54}Xe_{82} \rightarrow ^{136}_{56}Ba_{80}$	2457.83 ± 0.37	8.8573 ± 0.0044
$^{148}_{60}Nd_{88} \rightarrow ^{148}_{62}Sm_{86}$	1928.75 ± 1.92	5.756 ± 0.021
$^{150}_{60}Nd_{90} \rightarrow ^{150}_{62}Sm_{88}$	3371.38 ± 0.20	5.638 ± 0.028
$^{154}_{62}Sm_{92} \rightarrow ^{154}_{64}Gd_{90}$	1251.03 ± 1.25	22.75 ± 0.29
$^{160}_{64}Gd_{96} \rightarrow ^{160}_{66}Dy_{94}$	1729.69 ± 1.26	21.86 ± 0.19
$^{198}_{78}Pt_{120} \rightarrow ^{198}_{80}Hg_{118}$	1047.17 ± 3.11	7.36 ± 0.13

In this article, we report the results of our calculations in the nuclei listed in Table I. A selected number of decays was considered in [15] and preliminary results were presented in [16, 17]. Here we report the complete list of results divided into $0\nu\beta\beta$ (light neutrino exchange) and $0\nu_h\beta\beta$ (heavy neutrino exchange), Sect. II, and $2\nu\beta\beta$, Sect. III. By using these results we also set some limits on the mass of light $\langle m_\nu \rangle$ and heavy $\langle m_{\nu_h} \rangle$ neutrinos.

II. NEUTRINOLESS DOUBLEβ DECAY ($0\nu\beta\beta$)

A. Transition operator

The theory of $0\nu\beta\beta$ decay was first formulated by Furry [18] and further developed by Primakoff and Rosen [19], Molina and Pascual [20], Doi *et al.* [1], Haxton and Stephenson [21], and, more recently, by Tomoda [2] and Šimkovic *et al.* [3]. All these formulations often differ by factors of 2, by the number of terms retained in the non-relativistic expansion of the current and by their contribution. In order to have a standard set of calculations to be compared with QRPA and ISM, we adopt in this article the formulation of Šimkovic *et al.* [3]. The transition operator in momentum space, $p = |\vec{q}|$, is written as

$$T(p) = H(p) f(m_i, U_{ei}) \tag{5}$$

where for light-neutrino exchange

$$f(m_i, U_{ei}) = \frac{\langle m_\nu \rangle}{m_e}, \qquad \langle m_\nu \rangle = \sum_{k=light} (U_{ek})^2 m_k, \tag{6}$$

while for heavy neutrino exchange

$$\begin{aligned} f(m_i, U_{ei}) &= m_p \left\langle m_{\nu_h}^{-1} \right\rangle, \\ \left\langle m_{\nu_h}^{-1} \right\rangle &= \sum_{k=heavy} (U_{ek_h})^2 \frac{1}{m_{k_h}}. \end{aligned} \tag{7}$$

The (two-body) operator $H(p)$ can be written as

$$\begin{aligned} H(p) = \sum_{n,n'} \tau_n^\dagger \tau_{n'}^\dagger \left[-h^F(p) + h^{GT}(p) \vec{\sigma}_n \cdot \vec{\sigma}_{n'} \right. \\ \left. + h^T(p) S^p_{nn'} \right], \end{aligned} \tag{8}$$

with the tensor operator defined as

$$S^p_{nn'} = 3 \left[(\vec{\sigma}_n \cdot \hat{p}) (\vec{\sigma}_{n'} \cdot \hat{p}) \right] - \vec{\sigma}_n \cdot \vec{\sigma}_{n'}. \tag{9}$$

The Fermi (F), Gamow-Teller (GT) and tensor (T) contributions are given by

$$\begin{aligned} h^F(p) &= h^F_{VV}(p) \\ h^{GT}(p) &= h^{GT}_{AA}(p) + h^{GT}_{AP}(p) + h^{GT}_{PP}(p) + h^{GT}_{MM}(p) \\ h^T(p) &= h^T_{AP}(p) + h^T_{PP}(p) + h^T_{MM}(p). \end{aligned} \tag{10}$$

The terms AP-PP-MM are higher order corrections (HOC) arising from weak magnetism (M) and induced

pseudoscalar terms (P) in the weak nucleon current. The terms $h^{F,GT,T}(p)$ can be further factorized as

$$h^{F,GT,T}(p) = v(p)\tilde{h}^{F,GT,T}(p) \tag{11}$$

where $v(p)$ is called the neutrino "potential" and $\tilde{h}^{F,GT,T}(p)$ the "form factors". A list of form factors is given in Ref. [3] and recast in the form used by us in Table II. In this table, the finite nucleon size (FNS) is taken into account by taking the coupling constants g_V and g_A momentum dependent

$$\begin{aligned} g_V(p^2) &= g_V \frac{1}{\left(1+\frac{p^2}{M_V^2}\right)^2}, \\ g_A(p^2) &= g_A \frac{1}{\left(1+\frac{p^2}{M_A^2}\right)^2}. \end{aligned} \tag{12}$$

The value of M_V is well fixed by the electromagnetic form factor of the nucleon, $M_V^2 = 0.71(\mathrm{GeV/c^2})^2$ [22] and $g_V = 1$ by the hypothesis of conserved vector current (CVC). The value of M_A is estimated to be $M_A = 1.09(\mathrm{GeV/c^2})$ [23] and $g_A = 1.269$ [24].

Table II. Form factors in the formulation of [3] adapted to our calculation. m_p and m_π are the proton and pion mass and $\kappa_\beta = 3.70$ is the isovector anomalous magnetic moment of the nucleon.

Term	$\tilde{h}(p)$
$\tilde{h}^F_{VV}$	$g_A^2 \frac{(g_V^2/g_A^2)}{\left(1+p^2/M_V^2\right)^4}$
$\tilde{h}^{GT}_{AA}$	$\frac{g_A^2}{\left(1+p^2/M_A^2\right)^4}$
$\tilde{h}^{GT}_{AP}$	$g_A^2\left[-\frac{2}{3}\frac{1}{\left(1+p^2/M_A^2\right)^4}\frac{p^2}{p^2+m_\pi^2}(1-\frac{m_\pi^2}{M_A^2})\right]$
$\tilde{h}^{GT}_{PP}$	$g_A^2\left[\frac{1}{\sqrt{3}}\frac{1}{\left(1+p^2/M_A^2\right)^2}\frac{p^2}{p^2+m_\pi^2}\left(1-\frac{m_\pi^2}{M_A^2}\right)\right]^2$
$\tilde{h}^{GT}_{MM}$	$g_A^2\left[\frac{2}{3}\frac{g_V^2}{g_A^2}\frac{1}{\left(1+p^2/M_V^2\right)^4}\frac{\kappa_\beta^2 p^2}{4m_p^2}\right]$
$\tilde{h}^{T}_{AP}$	$-\tilde{h}^{GT}_{AP}$
$\tilde{h}^{T}_{PP}$	$-\tilde{h}^{GT}_{PP}$
$\tilde{h}^{T}_{MM}$	$\frac{1}{2}\tilde{h}^{GT}_{MM}$

The neutrino potential $v(p)$ is given, in the closure approximation, for light neutrino exchange by

$$v(p) = \frac{2}{\pi}\frac{1}{p\left(p+\tilde{A}\right)}. \tag{13}$$

For heavy neutrino exchange, the neutrino potential is given by

$$v(p) = \frac{2}{\pi}\frac{1}{m_e m_p}. \tag{14}$$

The contributions in momentum space, $h^{F,GT,T}(p)$, can be converted to the contributions in coordinate space, $h^{F,GT,T}(r)$, by taking the Fourier-Bessel transforms

$$\begin{aligned} h^{F,GT,T}(r) =& \frac{2}{\pi}\int_0^\infty j_\lambda(pr)\frac{1}{p\left(p+\tilde{A}\right)}\tilde{h}^{F,GT,T}(p) \\ & \times p^2 dp, \end{aligned} \tag{15}$$

for light-neutrino exchange and

$$\begin{aligned} h^{F,GT,T}(r) =& \frac{2}{\pi}\int_0^\infty j_\lambda(pr)\frac{1}{m_e m_p}\tilde{h}^{F,GT,T}(p) \\ & \times p^2 dp, \end{aligned} \tag{16}$$

for heavy neutrino exchange. Here $\lambda = 0$ for Fermi and Gamow-Teller contributions and $\lambda = 2$ for tensor contributions.

Finally, an additional improvement is the introduction of short range correlations (SRC). These can be taken into account by multiplying the potential $V(r)$ in coordinate space by a correlation function $f(r)$ squared. The most commonly used correlation function is the Jastrow function

$$f_J(r) = 1 - ce^{-ar^2}(1-br^2) \tag{17}$$

with $a = 1.1$ fm^{-2}, $b = 0.68$ fm^{-2} and $c = 1$ for the phenomenological Miller-Spencer parametrization [25], and, in recent years, the Argonne/CD-Bonn parametrizations [26] $a = 1.59/1.52$ fm^{-2}, $b = 1.45/1.88$ fm^{-2} and $c = 0.92/0.46$. Since our formulation is in momentum space, we take into account SRC by the Fourier-Bessel transform of $f_J(r)$.

In assessing the "goodness" of Šimkovic's formulation it is of interest to compare it with Tomoda's formulation. Apart from some differences in definitions, namely the fact that Tomoda defines the transition operator with a factor of 1/2 in front of Eq. (8), see Eq. (3.31) of Ref. [2], and the tensor operator with a factor of 1/3 in front of Eq. (9), see Eq. (3.54) of Ref. [2] and with a plus sign in front of the tensor operator in Eq. (8), in contrast with Eq. (13) of Ref. [3], and a nuclear radius $R = r_0 A^{1/3}$ with $r_0 = 1.2$ fm instead of $r_0 = 1.1$ fm of [3], differences which have caused, however, considerable confusion in the literature, the main difference between Tomoda's formulation and Šimkovic's formulation is that Tomoda considers more terms in $H(p)$, nine in all, 3GT, 3F, 1T, one pseudoscalar (P) and one recoil (R). Also, except for the terms $h_{VV}(p)$ and $h_{AA}(p)$, where the form factors and potentials coincide, all other form factors and potentials are different in Tomoda's formulation from Šimkovic's formulation. Although in this article we report results in the latter formulation, we note that we have results available for seven of the nine terms in Tomoda's formulation, 3GT, 3F, 1T. The form factors and potentials for these seven terms are listed in Table VIII of our Ref. [15]. In Table II of the same reference, we also show that the contribution of additional terms $\chi'_{GT}, \chi'_F, \chi'_T$ is not negligible and thus the assessment of the "goodness" of Šimkovic's formulation must reflect this point.

B. Matrix elements

We consider the decay of a nucleus ${}^{A}_{Z}\mathrm{X}_{N}$ into a nucleus ${}^{A}_{Z+2}\mathrm{Y}_{N-2}$. An example is shown in Fig. 3. The nuclear

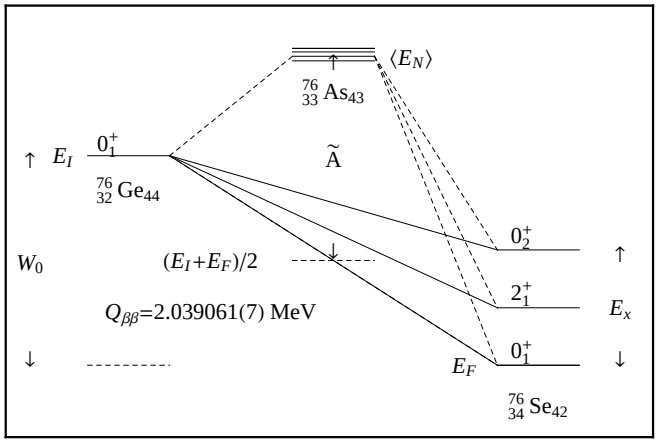

Figure 3. The decay ${}^{76}_{32}\mathrm{Ge}_{44} \rightarrow {}^{76}_{34}\mathrm{Se}_{42}$ is shown as an example of double-β decay.

matrix elements are those of the operator $H(p)$ of Eq. (8) between the ground state of the initial nucleus, and final state with angular momentum J_F

$$M_{0\nu} \equiv \left\langle {}^{A}\mathrm{X};0_1^+ \left| H(p) \right| {}^{A}\mathrm{Y};J_F \right\rangle . \tag{18}$$

If the decay proceeds through an s-wave, with two leptons in the final state we cannot form an angular momentum greater than one. We therefore calculate, in this article, only $0\nu\beta\beta$ matrix elements to final 0^+ states, the ground state 0_1^+, and the first excited state 0_2^+, for which, in a previous article [8] we have calculated the phase space factors. The form factors in Table II have a common factor of g_A^2, except $\tilde{h}^F_{VV}$. They depend on g_A^2 and g_V^2. We write

$$\begin{aligned} M_{0\nu} &= g_A^2 M^{(0\nu)}, \\ M^{(0\nu)} &= M^{(0\nu)}_{GT} - \left(\frac{g_V}{g_A}\right)^2 M^{(0\nu)}_{F} + M^{(0\nu)}_{T}, \end{aligned} \tag{19}$$

with the ratio g_V/g_A explicitly displayed in front of $M^{(0\nu)}_F$. The ratio g_V/g_A is also implicitly contained in $M^{(0\nu)}_{GT}$ and $M^{(0\nu)}_T$ through the terms $\tilde{h}^{GT}_{MM}$ and $\tilde{h}^{T}_{MM}$ (see Table II), and the matrix elements $M^{(0\nu)}_{GT}$, $M^{(0\nu)}_{F}$, and $M^{(0\nu)}_{T}$ are defined as

$$\begin{aligned} M^{(0\nu)}_{GT} &\equiv \left\langle {}^{A}\mathrm{X};0_1^+ \left| h^{GT}(p)/g_A^2 \right| {}^{A}\mathrm{Y};J_F \right\rangle , \\ M^{(0\nu)}_{F} &\equiv \left\langle {}^{A}\mathrm{X};0_1^+ \left| h^{F}(p)/g_V^2 \right| {}^{A}\mathrm{Y};J_F \right\rangle , \\ M^{(0\nu)}_{T} &\equiv \left\langle {}^{A}\mathrm{X};0_1^+ \left| h^{T}(p)/g_A^2 \right| {}^{A}\mathrm{Y};J_F \right\rangle . \end{aligned} \tag{20}$$

The reason for this separation is that the calculated single-β decay matrix elements of the GT operator in a particular nuclear model appear to be systematically larger than those derived from the measured ft values of the allowed GT transitions. The simplest way of taking into account this result is by introducing an effective $g_{A,eff}$, also sometimes written as $g_{A,eff} = qg_A$, where q is a quenching factor. The quenching of g_A will be discussed in Sect. III. Here we report results of the calculation of $M^{(0\nu)}$ in IBM-2 with the free values $g_V = 1$ and $g_A = 1.269$. These form the baseline for any discussion of NME in $0\nu\beta\beta$.

In order to evaluate the matrix elements we make use of the microscopic interacting boson model (IBM-2) [27]. The method of evaluation is discussed in detail in [15]. Here we briefly mention the logic of the method that is a mapping of the fermion operator H onto a boson space and its evaluation with bosonic wave functions. The mapping [28] can be done to leading order (LO), next to leading order (NLO), etc. . In Ref. [15] we showed, by explicit calculations, that NLO terms give, in general, negligible contribution, $\leq 1\%$. In this article, we present only LO calculations. The matrix elements of the mapped operators are then evaluated with realistic wave functions, taken either from the literature, when available, or obtained from a fit to the observed energies and other properties (B(E2) values, quadrupole moments, B(M1) values, magnetic moments,...). The values of the parameters used in the calculation are given in the Appendices. In Appendix A, we give the neutrino potential and its parameters. In Appendix B, we list the single-particle and -hole energies and strengths of interaction. In Appendix C, we give the parameters of the IBM-2 Hamiltonian for each nucleus considered in this article, together with their references. As shown in the references quoted in Appendix C, the quality of the IBM-2 wave functions ranges from very good to excellent for nuclei with $A \gtrsim 70$ where collective features are very pronounced, especially in deformed nuclei. As an example, we show in Fig. 4 a comparison between calculated and experimental spectra for the pair of nuclei ^{150}Nd - ^{150}Sm. For nuclei with $A \lesssim 70$, the IBM-2 description is only approximate, and one needs to go to the isospin conserving versions IBM-3 [29] and IBM-4 [30]. Nonetheless, we will report, for the sake of completeness, also results for ^{48}Ca decay, with the proviso that these are rather approximate. Also, in some cases, intruder configurations play a role, especially in the structure of the excited 0^+ state, and one needs to go to the configuration mixing version IBM2-CM [31]. All these improvements will be reported in subsequent papers.

C. Results

The matrix elements of the operator $H(p)$ have dimension fm^{-1}. It has become customary to quote the values of $M^{(0\nu)}$ by multiplying by the nuclear radius in fm, $R = R_0 A^{1/3}$, with $R_0 = 1.2$ fm. The matrix elements are then dimensionless.

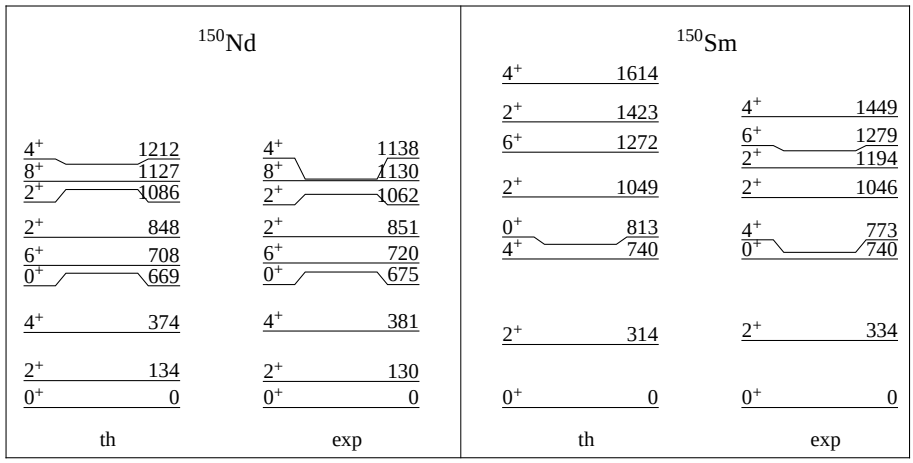

Figure 4. Comparison between calculated and experimental low-lying spectra for the pair of nuclei ^{150}Nd - ^{150}Sm.

1. $0\nu\beta\beta$ decay with light neutrino exchange

In Table III, we show the results of our calculation of the matrix elements to the ground state, 0_1^+, and first excited state, 0_2^+, broken down into GT, F and T contributions and their sum according to Eq. (19). We note that since we are covering all nuclei from $A = 76$ to $A = 198$, we have two classes of nuclei, those in which protons and neutrons occupy the same major shell ($A = 76, 82, 124, 128, 130, 136$) and those in which they occupy different major shells ($A = 96, 100, 110, 116, 148, 150, 154, 160, 198$). For example in $^{76}_{32}\mathrm{Ge}_{44} \rightarrow ^{76}_{34}\mathrm{Se}_{42}$ decay both protons and neutrons occupy the shell 28-50, while in $^{110}_{46}\mathrm{Pd}_{64} \rightarrow ^{110}_{48}\mathrm{Cd}_{62}$ decay protons occupy the shell 28-50, and neutrons occupy the shell 50-82. The magnitude of the Fermi matrix element which is related to the overlap of the proton and neutron wave functions is therefore different in these two classes of nuclei, being large in the former and small in the latter case. This implies a considerable amount of isospin violation for nuclei in the first class. The two classes are separated by lines in Table III in order to make the distinction clear. For completeness, we have added at the bottom of the table the IBM-2 calculation of ^{48}Ca$\rightarrow^{48}$Ti, assuming ^{48}Ca to be double magic. IBM-2 is rather poor in this case, as evidenced by the large Fermi matrix element, and the values in the table for ^{48}Ca$\rightarrow^{48}$Ti decay should be considered a rough estimate. Table III also shows the tensor matrix elements, $M_T^{(0\nu)}$. These are systematically small (about 5% of $M_{GT}^{(0\nu)}$) and have opposite or same sign than $M_{GT}^{(0\nu)}$ when protons and neutrons occupy the same major shell or not, respectively. This behavior can be traced to the fact that the neutrino "potential" $V(r)$ is different for tensor than for Fermi and Gamow-Teller. In the notation of Table VIII of Ref. [15], $V(r) = H(r)$ for Fermi and Gamow-Teller and $V(r) = -rH'(r)$ for tensor matrix elements.

A point of great interest is the comparison between various model calculations of the NME. Up to 2009, methods used were QRPA and ISM. In addition to these, there are now our calculation (IBM-2) and calculations based on DFT. Among the QRPA calculations there are those of the Tübingen group and those of the Jyväskylä group. These calculations often use different parametrizations of the short range correlations (SRC), include or not g_A^2 in $M^{(0\nu)}$, use different values of g_A, and are done in the closure or non-closure approximation. Therefore, the comparison between matrix elements in different models should be taken only as relative to a given matrix element, for example ^{76}Ge $\rightarrow^{76}$Se.

In Table IV we compare our results with those of a particular QRPA calculation, QRPA-Tü [13] and of a ISM calculation [14] with M-S parametrization of the SRC. The IBM-2 and QRPA-Tü results show a similar variation with A, while the ISM results are, apart from the small value in ^{48}Ca, clustered around ~ 2.00 in the entire range $A = 76 - 136$, and are a factor of approximately 2 smaller than IBM-2/QRPA-Tü. It should be noted that, due to the different approximation made in each model, a range of values would be more appropriate. For example, if we set to zero the Fermi matrix element in our calculated ^{48}Ca $\rightarrow^{48}$Ti decay, we obtain $M^{(0\nu)} = 1.33$ and thus our matrix elements should be more appropriately quoted as $M^{(0\nu)} = 1.33 - 1.98$. The sensitivity of the IBM-2 results to parameter changes, model assumptions and operator assumptions is further discussed in Sect. II C 3. The results in Table IV are summarized in Fig. 5, where they are plotted as a function of neutron number. The reason for this way of plotting is due to shell effects, as discussed in Sect. VI B of Ref. [15]. The matrix elements $M^{(0\nu)}$ attain their smallest values at the closed proton and neutron shells due to the form of the transition operator which for $\beta^-\beta^-$ decay annihilates a neutron pair and creates a proton pair. These shell ef-

Table III. IBM-2 nuclear matrix elements $M^{(0\nu)}$ (dimensionless) for $0\nu\beta\beta$ decay with Jastrow M-S SRC and $g_V/g_A = 1/1.269$.

	0_1^+				0_2^+			
A	$M_{GT}^{(0\nu)}$	$M_F^{(0\nu)}$	$M_T^{(0\nu)}$	$M^{(0\nu)}[0_1^+]$	$M_{GT}^{(0\nu)}$	$M_F^{(0\nu)}$	$M_T^{(0\nu)}$	$M^{(0\nu)}[0_2^+]$
76	4.10	-2.53	-0.25	5.42	1.81	-1.21	-0.10	2.46
82	3.26	-2.12	-0.25	4.37	0.86	-0.69	-0.05	1.23
96	2.26	-0.24	0.13	2.53	0.04	-0.00	0.00	0.04
100	3.32	-0.33	0.20	3.73	0.88	-0.09	0.05	0.99
110	3.22	-0.26	0.24	3.62	0.41	-0.04	0.03	0.46
116	2.49	-0.23	0.15	2.78	0.78	-0.06	0.04	0.85
124	2.69	-1.53	-0.13	3.50	2.03	-1.23	-0.10	2.70
128	3.46	-1.90	-0.16	4.48	2.44	-1.40	-0.10	3.22
130	3.12	-1.69	-0.14	4.03	2.33	-1.32	-0.09	3.07
136	2.59	-1.37	-0.11	3.33	1.40	-0.75	-0.04	1.82
148	1.73	-0.28	0.08	1.98	0.22	-0.04	0.01	0.25
150	2.03	-0.28	0.11	2.32	0.35	-0.05	0.02	0.39
154	2.23	-0.26	0.12	2.50	0.01	-0.01	0.01	0.02
160	3.25	-0.31	0.18	3.62	0.66	-0.08	0.05	0.75
198	1.64	-0.23	0.10	1.88	0.07	-0.01	0.01	0.08
48	1.53	-1.03	-0.19	1.98	3.62	-3.78	-0.13	5.83

Table IV. Nuclear matrix elements for $0\nu\beta\beta$ decay to ground state, 0_1^+, in IBM-2 with Jastrow M-S SRC and $g_A = 1.269$, QRPA-Tü with Jastrow M-S SRC and $g_A = 1.254$ [13], and ISM with Jastrow M-S SRC and $g_A = 1.25$ [14]. All matrix elements in dimensionless units.

		$M^{(0\nu)}$	
Decay	IBM-2	QRPA-Tü	ISM
^{48}Ca→^{48}Ti	1.98		0.54
^{76}Ge→^{76}Se	5.42	4.68	2.22
^{82}Se→^{82}Kr	4.37	4.17	2.11
^{96}Zr→^{96}Mo	2.53	1.34	
^{100}Mo→^{100}Ru	3.73	3.53	
^{110}Pd→^{110}Cd	3.62		
^{116}Cd→^{116}Sn	2.78	2.93	
^{124}Sn→^{124}Te	3.50		2.02
^{128}Te→^{128}Xe	4.48	3.77	2.26
^{130}Te→^{130}Xe	4.03	3.38	2.04
^{136}Xe→^{136}Ba	3.33	2.22	1.70
^{148}Nd→^{148}Sm	1.98		
^{150}Nd→^{150}Sm	2.32		
^{154}Sm→^{154}Gd	2.50		
^{160}Gd→^{160}Dy	3.62		
^{198}Pt→^{198}Hg	1.88		

Table V. Neutrinoless nuclear matrix elements to first excited state, 0_2^+, in IBM-2, QRPA-Tü RCM/BEM [32], and ISM [33]. All matrix elements in dimensionless units.

		$M^{(0\nu)}$	
Decay	IBM-2	QRPA-Tü	ISM
^{48}Ca→^{48}Ti	5.83		0.68
^{76}Ge→^{76}Se	2.46	1.28/0.99	1.49
^{82}Se→^{82}Kr	1.23*	1.34/0.95*	0.28*
^{96}Zr→^{96}Mo	0.04		
^{100}Mo→^{100}Ru	0.99	1.27/1.76	
^{110}Pd→^{110}Cd	0.46		
^{116}Cd→^{116}Sn	0.85		
^{124}Sn→^{124}Te	2.70		0.80
^{128}Te→^{128}Xe	3.22*		
^{130}Te→^{130}Xe	3.07		0.19
^{136}Xe→^{136}Ba	1.82	4.42/0.44	0.49
^{148}Nd→^{148}Sm	0.25		
^{150}Nd→^{150}Sm	0.39		
^{154}Sm→^{154}Gd	0.02		
^{160}Gd→^{160}Dy	0.75		
^{198}Pt→^{198}Hg	0.08*		

* Negative Q-value

fects are very clear in both IBM-2 and QRPA calculations, and to some extent also in the ISM calculation. They are responsible for the small matrix element in the decay of the doubly magic nucleus ^{48}Ca. They are also responsible for the ratio of the matrix elements of two different isotopes of the same element. For example, a simple calculation using the pair operators of Ref. [15], Eq. (42) gives $M^{(0\nu)}(^{128}\mathrm{Te})/M^{(0\nu)}(^{130}\mathrm{Te}) = 1.11$ to be compared with IBM-2, 1.11, QRPA-Tü, 1.13, and ISM, 1.11.

Our results to 0_2^+ are shown in Table V. Because of the reduced phase space factor for decay to 0_2^+, this table is of less interest. In this case, there appears to be no correlation between IBM-2 and other calculations. It should noted, however, that the QRPA-Tü results shown in Table V were done before an error was discovered in the treatment of short range correlations [34] and with two different methods for treating the excited 0_2^+ state, recoupling method (RCM) and boson expansion method (BEM) [32]. These results are therefore inconsistent by a factor of approximately 2 with those in Table IV and Ref. [13] for 0_1^+. Also, IBM-2 calculations have been done

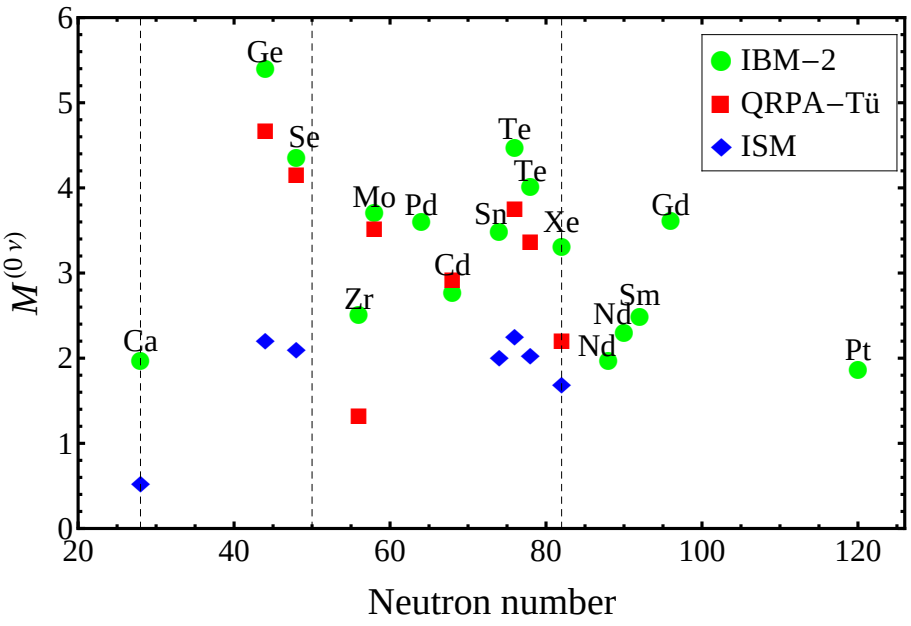

Figure 5. (Color online) IBM-2 results for $0\nu\beta\beta$ compared with QRPA-Tü [13] and ISM [14].

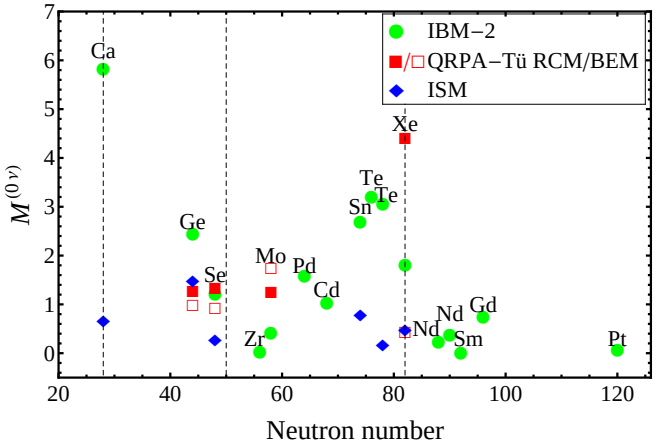

Figure 6. (Color online) IBM-2 results for $0\nu\beta\beta$ decay to 0_2^+ compared with QRPA-Tü [32] and ISM [33].

without including intruder configurations. It is known that, in some cases, the 0_2^+ state is an intruder state. Most notable cases are Ge, Mo, Cd, Nd, and Hg isotopes [35, p.180]. Although configuration mixing IBM-2 calculations for these nuclei are available, they have not been implemented yet in the calculation of $0\nu\beta\beta$ to 0_2^+ states. The comparison between IBM-2, QRPA-Tü, and ISM is shown in Fig. 6

The most detailed comparison between different model calculations yet has been done recently by Suhonen [36]. This author has shown a very close correspondence between the IBM-2 results and the pnQRPA-Jy result, Table VI, and has argued that the reason why QRPA and IBM-2 agree is due to the fact that QRPA can be seen as a leading order boson expansion. This statement should be taken, however, with caution since QRPA results require the adjustment of the parameter g_{pp}.

Table VI. Comparison between IBM-2 and QRPA-Jy [36] nuclear matrix elements $M^{(0\nu)}$ (dimensionless) for $0\nu\beta\beta$ decay.

	0_1^+		0_2^+	
A	IBM-2	QRPA	IBM-2	QRPA
48	1.98	1.09-1.89	5.83	
76	5.42	2.28-4.17	2.46	2.47-5.38
82	4.37	2.11-3.51	1.23	0.831-1.85
96	2.53	2.00-2.07	0.04	1.96
100	3.73	2.26-2.74	0.99	0.31
110	3.62	3.63-4.51	0.46	0.96-1.73
116	2.78	2.36-3.98	0.85	0.25
124	3.50	2.58-4.18	2.70	3.96-5.88
128	4.48	2.74-4.15	3.22	
130	4.03	2.60-3.78	3.07	3.88-6.61
136	3.33	1.83-2.53	1.82	2.75-6.08

Another question which has been extensively analyzed in recent months is the size of the Fermi matrix elements, and its comparison between different models. To this end, it is convenient to introduce the quantity $\chi_F = (g_V/g_A)^2 M_F^{(0\nu)}/M_{GT}^{(0\nu)}$. This quantity is shown in Table VII. One can see that the situation is more complex than in the case of the overall matrix elements, due to the different approximations made by the different models. The IBM-2 results are large for nuclei in which

protons and neutrons occupy the same major shells, but small in cases in which protons and neutrons occupy different major shells. For QRPA-Jy they are uniformly large ($\chi_F \sim -0.30$) while for ISM they are uniformly small ($\chi_F \sim -0.15$).

The large Fermi matrix elements in IBM-2 with protons and neutrons in the same major shell and in QRPA throughout point out to large isospin violation in the wave functions of the initial and final nuclei. In the case of $2\nu\beta\beta$ decay, if isospin is a good quantum number, the Fermi matrix elements should identically vanish. By a similar argument, the Fermi matrix elements in $0\nu\beta\beta$ are expected to be small, although not zero, the main difference between $2\nu\beta\beta$ and $0\nu\beta\beta$ being the neutrino "potential", given in Appendix A, Table XIX. For this reason, the calculated values of χ_F given in Table VII may be entirely spurious and should be considered with a large error. It is difficult to estimate the error in χ_F introduced by isospin violation, since there are no direct experimental data for single-β $0^+ \to 0^+$ transitions from odd-odd to even-even (or vice versa) in heavy nuclei. The estimate of the error also depends on which nucleus is considered. The maximum error is 100%, if the Fermi matrix elements are entirely spurious, in which case the values of Table VII should be quoted as $-0.42(42)$ for ^{48}Ca and similarly for all others. Another estimate is to extract the error by comparing with ISM calculations which have the smallest values of χ_F, in which case the quoted value should be $-0.42(28)$ with an error of 67%. We have used this estimate of the error in the following subsection 3 and in Table XII.

Table VII. Comparison between Fermi matrix elements, χ_F, in IBM-2, QRPA-Jy [37] and ISM [38].

Decay	χ_F IBM-2	χ_F QRPA-Jy	χ_F ISM
^{48}Ca	-0.42	-0.56[a]	-0.14
^{76}Ge	-0.38	-0.22	-0.10
^{82}Se	-0.42	-0.28	-0.10
^{96}Zr	-0.06	-0.43	
^{100}Mo	-0.06	-0.40	
^{110}Pd	-0.05	-0.38	-0.16
^{116}Cd	-0.06	-0.28	-0.19
^{124}Sn	-0.35	-0.42	-0.13
^{128}Te	-0.34	-0.37	-0.13
^{130}Te	-0.34	-0.37	-0.13
^{136}Xe	-0.33	-0.34	-0.13
^{148}Nd	-0.10		
^{150}Nd	-0.09		
^{154}Sm	-0.07		
^{160}Gd	-0.06		
^{198}Pt	-0.09		

[a] Ref. [39]

In addition to the calculations discussed above, several others have been done, most notably in the deformed QRPA [40, 41] and in the projected HFB framework [42], and the energy density functional method [43]. Since these use SRC with Argonne/CD-Bonn and UCOM they will be discussed at the end of Sect. II C 3.

2. $0\nu\beta\beta$ decay with heavy neutrino exchange

These matrix elements can be simply calculated by replacing the potential $v(p) = 2\pi^{-1}[p(p+\tilde{A})]^{-1}$ of Eq. (13) with the potential $v_h(p) = 2\pi^{-1}(m_e m_p)^{-1}$ of Eq. (14). Table VIII gives the corresponding matrix elements. The index "h" distinguishes these matrix elements from those with light neutrino exchange. Our results are compared with QRPA-Tü results in Table IX. These QRPA results are obtained with Jastrow SRC [3] and prior to the more refined treatment of SRC of Ref. [13], and are shown here for the sake of comparison of the A dependence, not of their absolute magnitude which is a factor of approximately 2 smaller than in IBM-2. It has been suggested that measurement of neutrinoless double-β decay in different nuclei may be used to distinguish between the two mechanisms, light or heavy neutrino exchange. However, the results in Table III and Table IX are highly correlated as it is clear from the fact that they are obtained one from the other by replacing the potential $v(p)$ with $v_h(p)$. Therefore, this criterion cannot be used to distinguish between the two mechanisms [45].

3. Sensitivity to parameter changes, model assumptions and operator assumptions

Many ingredients go into the calculation of the nuclear matrix elements. In Ref. [15], the sensitivity to input parameter changes was estimated to be: (1) Single particle energies. This sensitivity was emphasized in Ref. [46] within the framework of QRPA and has been the subject of several experimental investigations [47, 48]. We estimate it to be 10%. (2) Strengths of interactions, in the present case the surface delta interaction used to calculate the structure of the pair states. We estimate this to be 5%. We note that this is the main source of sensitivity in QRPA, especially in nuclei close to the spherical-deformed transition, for example ^{150}Nd. (3) Oscillator parameter in the single particle wave functions. We estimate this to be 5%. (4) Closure energy in the neutrino potential. We estimate this to be 5%. (5) Nuclear radius. If the matrix elements are quoted in dimensionless units there is also the sensitivity to R. We estimate this to be 5%. However, this sensitivity can be reduced to a small value, 1%, if the experimental rms value is used instead of the formula $R = R_0 A^{1/3}$. The total estimated sensitivity to input parameters is 30% if all contributions are added or 14% if combined in quadrature.

Table VIII. Nuclear matrix elements for the heavy neutrino exchange mode of the neutrinoless double-β decay to the ground state (columns 2,3,4, and 5) and to the first excited state (columns 6,7,8, and 9) using the microscopic interacting boson model (IBM-2) with Jastrow M-S SRC and $g_V/g_A = 1/1.269$.

	0_1^+				0_2^+			
A	$M_{GT_h}^{(0\nu)}$	$M_{F_h}^{(0\nu)}$	$M_{T_h}^{(0\nu)}$	$M_h^{(0\nu)}[0_1^+]$	$M_{GT_h}^{(0\nu)}$	$M_{F_h}^{(0\nu)}$	$M_{T_h}^{(0\nu)}$	$M_h^{(0\nu)}[0_2^+]$
76	52.5	-39.5	-29.0	48.1	19.5	-15.4	-10.5	18.5
82	43.9	-33.9	-29.4	35.6	8.53	-7.36	-4.96	8.14
96	33.6	-18.8	13.6	59.0	0.700	-0.382	0.321	1.26
100	54.5	-30.0	26.1	99.3	4.59	-2.55	1.70	7.87
110	49.3	-26.5	29.9	95.7	18.4	-9.73	10.0	34.5
116	36.4	-20.1	18.2	67.1	13.9	-7.72	7.07	25.8
124	37.0	-27.1	-16.1	37.8	25.2	-19.0	-10.6	26.4
128	47.0	-34.1	-19.7	48.4	28.0	-21.1	-11.1	30.0
130	42.7	-30.9	-17.9	44.0	25.9	-19.6	-10.0	28.1
136	33.7	-24.3	-13.7	35.1	12.9	-9.90	-4.39	14.7
148	35.8	-21.2	10.4	59.4	3.99	-2.43	1.07	6.57
150	39.9	-23.0	14.2	68.4	5.90	-3.42	1.90	9.92
154	38.6	-21.8	14.9	67.1	1.93	-1.12	1.20	3.82
160	51.9	-28.7	23.2	92.9	13.1	-7.34	6.65	24.3
198	34.7	-20.8	13.8	61.5	1.51	-0.899	0.688	2.76
48	26.8	-20.1	-22.9	16.3	23.8	-27.3	-6.95	33.8

Table IX. Neutrinoless nuclear matrix elements to ground state, 0_1^+, in IBM-2 and QRPA-Tü [3] for the heavy neutrino exchange mode and M-S SRC. All matrix elements are in dimensionless units.

	$M_h^{(0\nu)}$	
Decay	IBM-2	QRPA-Tü
^{48}Ca→^{48}Ti	16.3	
^{76}Ge→^{76}Se	48.1	32.6
^{82}Se→^{82}Kr	35.6	30.0
^{96}Zr→^{96}Mo	59.0	14.7
^{100}Mo→^{100}Ru	99.3	29.7
^{110}Pd→^{110}Cd	95.7	
^{116}Cd→^{116}Sn	67.1	21.5
^{124}Sn→^{124}Te	37.8	
^{128}Te→^{128}Xe	48.4	26.6
^{130}Te→^{130}Xe	44.0	23.1
^{136}Xe→^{136}Ba	35.1	14.1
^{148}Nd→^{148}Sm	59.4	
^{150}Nd→^{150}Sm	68.4	35.6
^{154}Sm→^{154}Gd	67.1	
^{160}Gd→^{160}Dy	92.9	
^{198}Pt→^{198}Hg	61.5	

In addition, we estimate the sensitivity to model assumptions to be: (1) Truncation to S-D space. We estimate this to be ranging from 1% in spherical nuclei to 10% in deformed nuclei. (2) Isospin purity. We estimate this to be small, 1%, for GT and T matrix elements, and large, 10%, for F matrix elements. Taking into account the fact that the F matrix elements contribute only ∼20% to the total matrix elements, we estimate the total sensitivity to model assumptions to be ranging from 3% in spherical nuclei, to 12% in deformed nuclei (in addition) or 2%-10% (in quadrature). A special case is that of ^{48}Ca decay for which, for reasons mentioned above, the Fermi matrix elements are overestimated. In this case the sensitivity to model assumptions may be as high as 20% (in addition) or 16% (in quadrature).

Finally, there is the estimated sensitivity to operator assumptions: (1) Form of the transition operator. We have already commented in Sect. II. A on the differences between Šimkovic's [3] and Tomoda's [2] formulations. This is a source of considerable uncertainty. We estimate the sensitivity to 5% by comparing our calculations using Tomoda's and Šimkovic's formulations. However, there still remains the question of the recoil contribution which was a source of major disagreement in early calculations. (2) Finite nuclear size (FNS). We estimate this to be small, 1%, due to the fact that we have used realistic nucleon form factors with parameters determined from experiment. (3) Short range correlations (SRC). The sensitivity to the form of short range correlations has been very recently the subject of many studies. To investigate this point, we have done calculations with three different types of correlations, (a) Jastrow Miller-Spencer (MS) and (b/c) Argonne/CD-Bonn (CCM). The results are shown in Table X, where we also show a comparison with results of calculations in QRPA and ISM using M–S, CCM and the unitary correlation operator method (UCOM) [49]. It appears that in going from M–S to CCM or UCOM the matrix elements in all three methods (IBM-2, QRPA, ISM) increase. In IBM-2 the multiplicative factor when going from M–S to CCM–Argonne is 1.10-1.20. In QRPA-Tü it is 1.21-1.42 from M–S to CCM-Argonne and 1.21-1.33 from M–S to UCOM. In ISM the factor is 1.25-1.30 from M–S to UCOM. This multiplicative factor was taken into account in Ref. [50] when comparing IBM-2 matrix elements with ISM. The

Table X. Comparison between matrix elements $M^{(0\nu)}$ calculated with Miller-Spencer (M-S) and Argonne/CD-Bonn (CCM) in IBM-2, with M-S, CCM and UCOM in QRPA-Tü [13, 26, 41] and with M-S and UCOM in ISM [14, 33]. Note that the QRPA matrix elements are evaluated using $g_A = 1.254$ and the ISM matrix elements are evaluated using $g_A = 1.25$.

	IBM-2		QRPA-Tü			ISM	
A	M-S	CCM	M-S[a]	CCM[b]	UCOM[a]	M-S[c]	UCOM[d]
48	1.98	2.28/2.38				0.59	0.85
76	5.42	5.98/6.16	4.68	5.81/6.32	5.73	2.22	2.81
82	4.37	4.84/4.99	4.17	5.19/5.65	5.09	2.11	2.64
96	2.53	2.89/3.00	1.34	1.90/2.09	1.79		
100	3.73	4.31/4.50	3.52	4.75/5.25	4.58		
110	3.62	4.15/4.31					
116	2.78	3.16/3.29	2.93	3.54/3.99	3.54		
124	3.50	3.89/4.02				2.02	2.62
128	4.48	4.97/5.13	3.77	4.93/5.49	4.76	2.26	2.88
130	4.03	4.47/4.61	3.38	4.37/4.92	4.26	2.04	2.65
136	3.33	3.67/3.79	2.22	2.78/3.11	2.76	1.70	2.19
148	1.98	2.36/2.49					
150	2.32	2.74/2.88		3.34[e]			
154	2.50	2.91/3.04					
160	3.62	4.17/4.34		3.76[e]			
198	1.88	2.25/2.37					

[a] Ref. [13]
[b] Ref. [26]
[c] Ref. [14]
[d] Ref. [33]
[e] Ref. [41]

discrepancy between IBM-2 and QRPA-Tü multiplicative factors is not understood and should be investigated further. In Table X, we have also added recent calculations in deformed QRPA for decay of ^{150}Nd and ^{160}Gd [41]. One may note that the correspondence between QRPA and IBM-2 persists even in deformed nuclei.

The total estimated sensitivity is here 11% (addition) or 7% (quadrature), assuming no recoil contribution to the matrix elements. Combining all, we have a total estimated sensitivity of 44%-55% if all the contributions are added or 16%-19% if they are combined in quadrature.

The short range correlations affect $0\nu_h\beta\beta$ decay differently than $0\nu\beta\beta$. We have therefore investigated the dependence of $0\nu_h\beta\beta$ matrix elements with M-S, and CCM correlations. The results are shown in Table XI. We see here an increase of a factor of 1.69-2.80 when going from M–S to Argonne/CD-Bonn. This is due to the fact that, as remarked in Appendix A, the neutrino potential for heavy neutrino exchange is a contact interaction in configuration space and thus strongly influenced by SRC. The correlation function in (17) has a value $f_J(0) = 1-c$ at $r = 0$. For the M–S parametrization $c = 1$, $f_J(0) = 0$, and thus, in the absence of a nucleon form factor, the matrix elements $M_h^{(0\nu)}$ vanish. The Argonne/CD-Bonn parametrizations have $c = 0.92/0.46$ and thus a nonzero value at $r = 0$. These results are modified by the presence of the nucleon form factors of (12), and the final results depend strongly on the choice of $g_V(p^2)$ and $g_A(p^2)$. From Table XI, columns 4 and 5, it appears that the increase in the matrix elements when going from M–S to CCM-Argonne in QRPA-Tü is much larger, 7.01-10.1, than in IBM-2. As in the case of light neutrino exchange, this discrepancy is not understood and should be investigated further. The large increase both in IBM-2 and QRPA also points to the strong sensitivity of the calculated $0\nu_h\beta\beta$ matrix elements to the specific form of SRC, and thus to the fact that the treatment here and in other calculations in the literature, through the nucleon form factors, may not be satisfactory. A more consistent treatment is discussed in Refs. [51, 52]. In view of all these problems, we estimate the sensitivity to SRC for $0\nu_h\beta\beta$ decay to be much larger (50%) than that for $0\nu\beta\beta$ decay (5%). The total estimated sensitivity to operator assumptions for $0\nu_h\beta\beta$ is then 56% (addition) and 50% (quadrature).

To summarize the situation we show in Table XII our final results with M-S SRC, together with an estimate of the error, based on the arguments given above. The error estimate is 30% in ^{48}Ca, 19% in nuclei with protons and neutrons in the same major shell and 16% in nuclei with protons and neutrons in different major shells, for $0\nu\beta\beta$. For $0\nu_h\beta\beta$, our estimated error is dominated by SRC. In Table XII we have used 58% in ^{48}Ca, 53% in nuclei with protons and neutrons in the same major shell and 52% in nuclei with protons and neutrons in different major shells.

Finally, having investigated the effect of short range correlations on $0\nu\beta\beta$ we are now able to compare our results with all available calculations done with the same SRC including DFT [43] and HFB [42]. These are shown

Table XI. Comparison between $M_h^{(0\nu)}$ matrix elements calculated with different Jastrow parametrizations for the SRC: Miller-Spencer and CCM (Argonne and CD-Bonn) in IBM-2 and QRPA-Tü [3, 53].

A	IBM-2		QRPA-Tü	
	M-S	CCM	M-S[a]	CCM[b]
48	16.3	46.3/76.0		
76	48.1	107/163	32.6	233/351
82	35.6	84.4/132	30.0	226/340
96	59.0	99.0/135	14.7	
100	99.3	165/224	29.7	250/388
110	95.7	155/208		
116	67.1	110/149	21.5	
124	37.8	79.6/120		
128	48.4	101/152	26.6	
130	44.0	92.0/138	23.1	234/364
136	35.1	72.8/109	14.1	
148	59.4	103/142		
150	68.4	116/160	35.6	
154	67.1	113/155		
160	92.9	155/211		
198	61.5	104/141		

[a] Ref. [3]
[b] Ref. [53]

Table XII. Final IBM-2 matrix elements with M-S SRC and error estimate.

Decay	Light neutrino exchange	Heavy neutrino exchange
^{48}Ca	1.98(59)	16.3(95)
^{76}Ge	5.42(103)	48.1(255)
^{82}Se	4.37(83)	35.6(189)
^{96}Zr	2.53(40)	59.0(309)
^{100}Mo	3.73(60)	99.3(516)
^{110}Pd	3.62(58)	95.7(498)
^{116}Cd	2.78(44)	67.1(321)
^{124}Sn	3.50(67)	37.8(200)
^{128}Te	4.48(85)	48.4(257)
^{130}Te	4.03(77)	44.0(233)
^{136}Xe	3.33(63)	35.1(186)
^{148}Nd	1.98(32)	59.4(309)
^{150}Nd	2.32(37)	68.4(356)
^{154}Sm	2.50(40)	67.1(349)
^{160}Gd	3.62(58)	92.9(483)
^{198}Pt	1.88(30)	61.5(320)

in Fig. 7. We note now that while ISM/QRPA/IBM-2 have the same trend with A, the other two do not. For the isotopic ratio $M^{(0\nu)}(^{128}\text{Te})/M^{(0\nu)}(^{130}\text{Te})$ the DFT method gives 0.86 in sharp contrast with the value 1.11. Also, while ISM/QRPA/IBM-2 have a small value for ^{96}Zr, DFT has a large value. We therefore conclude that the approximations made in the DFT/HFB lead to a different behavior with A. This point is currently being investigated [44]. Also, the Fermi matrix elements in DFT are comparable to those in IBM-2 and larger than in the ISM [44].

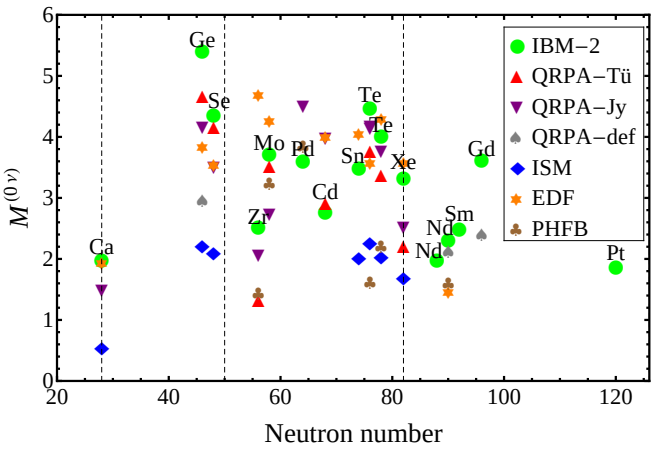

Figure 7. (Color online) IBM-2 results for $0\nu\beta\beta$ nuclear matrix elements compared with QRPA-Tü [13], ISM [14], QRPA-Jy [36, 54–56], QRPA-deformed [41], DFT [43], and HFB [42].

D. Limits on neutrino mass

1. *Light neutrino exchange*

The calculation of nuclear matrix elements in IBM-2 can now be combined with the phase space factors calculated in [8] and given in Table III and Fig. 8 of that reference to produce our final results for half-lives for light neutrino exchange in Table XIII and Fig. 8. The half-lives are calculated using the formula

$$[\tau_{1/2}^{0\nu}]^{-1} = G_{0\nu}^{(0)} \left|M_{0\nu}\right|^2 \left|\frac{\langle m_\nu \rangle}{m_e}\right|^2 . \qquad (21)$$

We note here that the combination must be done consistently. If the value of g_A is included in $M_{0\nu}$, then it should not be included in $G_{0\nu}^{(0)}$. Similarly for a factor of 4 included in some definition of $G_{0\nu}^{(0)}$ [2] and not in others [57]. See Eq. (53) of Ref. [8]. This point has caused considerable confusion in the literature. In Table XIII and Fig. 8 the values $\langle m_\nu \rangle = 1$ eV and $g_A = 1.269$ are used. For other values they can be scaled with $\left|\langle m_\nu \rangle / m_e\right|^2$ and g_A^4.

The effective neutrino mass is the quantity we want to extract from experiment. Unfortunately, the axial vector coupling constant is renormalized in nuclei to $g_{A,eff}$. A (model dependent) estimate of $g_{A,eff}$ can be obtained from the experimental knowledge of single-β decay and/or of $2\nu\beta\beta$ decay. This will be discussed in the following section. Here we show in Fig. 9 and Table XIII, the limits on neutrino mass from current experimental upper limits using IBM-2 matrix elements of Table V and $g_A = 1.269$. In addition to the experimental upper

Table XIII. Left: Calculated half-lives in IBM-2 M-S SRC for neutrinoless double-β decay for $\langle m_\nu \rangle = 1$ eV and $g_A = 1.269$. Right: Upper limit on neutrino mass from current experimental limit from a compilation of Barabash [58]. The value reported by Klapdor-Kleingrothaus *et al.* [59], IGEX collaboration [60], and the recent limits from KamLAND-Zen [61] and EXO [62] are also included.

Decay	$\tau^{0\nu}_{1/2}(10^{24}\text{yr})$	$\tau^{0\nu}_{1/2,exp}(\text{yr})$	$\langle m_\nu \rangle$ (eV)
^{48}Ca→^{48}Ti	1.03	$> 5.8 \times 10^{22}$	< 4.2
^{76}Ge→^{76}Se	1.45	$> 1.9 \times 10^{25}$	< 0.28
		1.2×10^{25} [a]	0.35
		$> 1.6 \times 10^{25}$ [b]	< 0.30
^{82}Se→^{82}Kr	0.52	$> 3.6 \times 10^{23}$	< 1.2
^{96}Zr→^{96}Mo	0.77	$> 9.2 \times 10^{21}$	< 9.1
^{100}Mo→^{100}Ru	0.46	$> 1.1 \times 10^{24}$	< 0.64
^{110}Pd→^{110}Cd	1.60		
^{116}Cd→^{116}Sn	0.78	$> 1.7 \times 10^{23}$	< 2.1
^{124}Sn→^{124}Te	0.91		
^{128}Te→^{128}Xe	8.53	$> 1.5 \times 10^{24}$	< 2.4
^{130}Te→^{130}Xe	0.44	$> 2.8 \times 10^{24}$	< 0.39
^{136}Xe→^{136}Ba	0.62	$> 5.7 \times 10^{24}$ [c]	< 0.33
		$> 1.6 \times 10^{25}$ [d]	< 0.20
^{148}Nd→^{148}Sm	2.54		
^{150}Nd→^{150}Sm	0.30	$> 1.8 \times 10^{22}$	< 4.1
^{154}Sm→^{154}Gd	5.34		
^{160}Gd→^{160}Dy	0.80		
^{198}Pt→^{198}Hg	3.77		

[a] Ref. [59]
[b] Ref. [60]
[c] Ref. [61]
[d] Ref. [62]

limits, a value has been reported for the half-life in ^{76}Ge, 1.2×10^{25}yr [59]. This is also reported in Fig. 9.

The average light neutrino mass is constrained by atmospheric, solar, reactor and accelerator neutrino oscillation experiments to be [75]

$$\begin{aligned} \langle m_\nu \rangle &= \left| c_{13}^2 c_{12}^2 m_1 + c_{13}^2 s_{12}^2 m_2 e^{i\varphi_2} + s_{13}^2 m_3 e^{i\varphi_3} \right|, \\ c_{ij} &= \cos\vartheta_{ij}, \quad s_{ij} = \sin\vartheta_{ij}, \quad \varphi_{2,3} = [0, 2\pi], \\ \left(m_1^2, m_2^2, m_3^2\right) &= \frac{m_1^2 + m_2^2}{2} \\ &\quad + \left(-\frac{\delta m^2}{2}, +\frac{\delta m^2}{2}, \pm \Delta m^2 \right). \end{aligned} \tag{22}$$

Using the best fit values [75]

$$\begin{aligned} &\sin^2\vartheta_{12} = 0.213, \quad \sin^2\vartheta_{13} = 0.016, \\ &\sin^2\vartheta_{23} = 0.466, \quad \delta m^2 = 7.67 \times 10^{-5}\ \text{eV}^2, \\ &\Delta m^2 = 2.39 \times 10^{-3}\ \text{eV}^2 \end{aligned} \tag{23}$$

we obtain the values given in Fig. 10. In this figure we have added the current limits, for $g_A = 1.269$, coming from CUORICINO [63], IGEX [60], NEMO-3 [64], KamLAND-Zen [61], and EXO [62] experiment. Also, we use in this section II D, and in the rest of the article, c=1, to conform with standard notation.

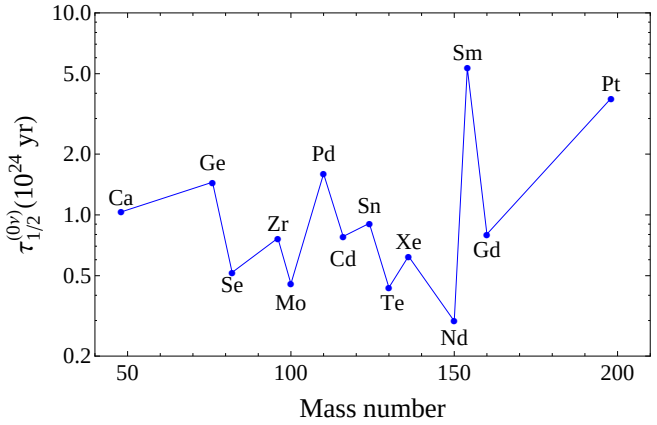

Figure 8. (Color online) Expected half-lives for $\langle m_\nu \rangle = 1$ eV, $g_A = 1.269$. The points for ^{128}Te and ^{148}Nd decays are not included in this figure. The figure is in semilogarithmic scale.

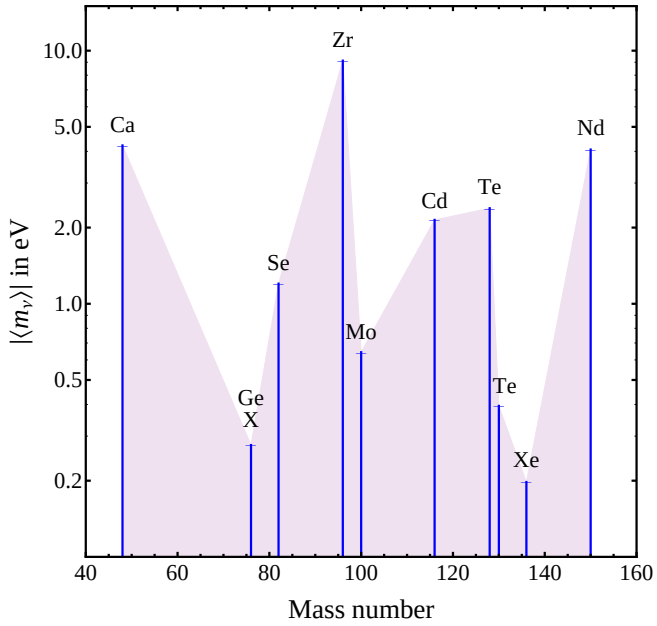

Figure 9. (Color online) Limits on neutrino mass from current experimental limits from a compilation of A. Barabash [58] and recent measurement for ^{136}Xe from EXO [62]. The value reported by Klapdor-Kleingrothaus *et al.* [59] is shown by the symbol X. The figure is in semilogarithmic scale. The shaded area represents the values of $|\langle m_\nu \rangle|$ allowed by the current experiments.

2. *Heavy neutrino exchange*

The half-lives for this case are calculated using the formula

$$\begin{aligned} [\tau^{0\nu_h}_{1/2}]^{-1} &= G^{(0)}_{0\nu} \left| M_{0\nu_h} \right|^2 |\eta|^2 \\ \eta &\equiv m_p \left\langle m^{-1}_{\nu_h} \right\rangle = \sum_{k=heavy} (U_{ek_h})^2 \frac{m_p}{m_{k_h}}. \end{aligned} \tag{24}$$

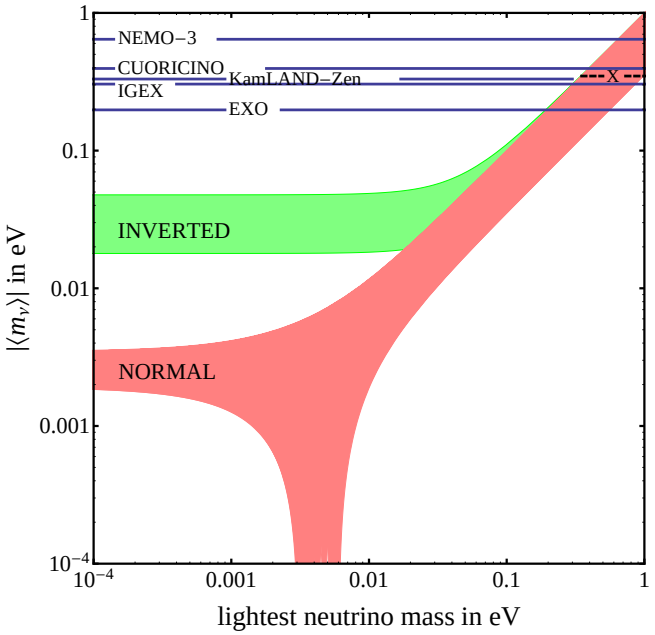

Figure 10. (Color online) Current limits to $\langle m_\nu \rangle$ from CUORICINO [63], IGEX [60], NEMO-3 [64], KamLAND-Zen [61], and EXO [62], and IBM-2 M-S SRC nuclear matrix elements. The value of Ref. [59] is shown by X. It is consistent only with nearly degenerate neutrino masses. The figure is in logarithmic scale.

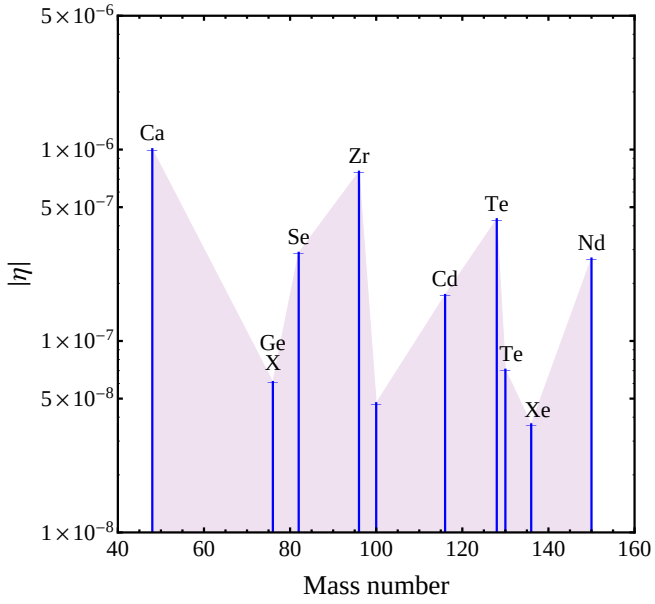

Figure 11. (Color online) Limits on the lepton nonconserving parameter $|\eta|$. The value of Ref. [59] is shown by X. The figure is in semilogarithmic scale. The shaded area represents the values of $|\eta|$ allowed by the current experiments.

The expected half-lives for $|\eta| = 2.75 \times 10^{-7}$, and using the IBM-2 matrix elements of Table IX, are shown in Table XIV. For other values of η they scale as $|\eta|^2$. There are no direct experimental bounds on η. Recently, Tello *et al.* [7] have argued that from lepton flavor violating processes and from large hadron collider (LHC) experiments one can put some bounds on the right-handed leptonic mixing matrix $U_{ek,heavy}$ and thus on η. In the model of Ref. [7], when converted to our notation, η can be written as

$$\eta = \frac{M_W^4}{M_{WR}^4} \sum_{k=heavy} (V_{ek_h})^2 \frac{m_p}{m_{k_h}}, \qquad (25)$$

where M_W is the mass of the W-boson, $M_W = (80.41 \pm 0.10)$ GeV [24], M_{WR} is the mass of WR-boson, assumed in [7] to be $M_{WR} = 3.5$ TeV and $V = (M_{WR}/M_W)^2 U$. The ratio $(M_W/M_{WR})^4$ is then 2.75×10^{-7}, the value we have used in Table XIV left. By comparing the calculated half-lives with their current experimental limits, we can set limits on the lepton nonconserving parameter $|\eta|$, shown in Table XIV and Fig. 11.

If we write

$$\eta = \frac{M_W^4}{M_{WR}^4} \frac{m_p}{\langle m_{\nu_h} \rangle}, \qquad (26)$$

we can also set limits on the average heavy neutrino mass, $\langle m_{\nu_h} \rangle$, as shown in the last column of Table XIV. This limit is model dependent since it is assumed that $M_{WR} = 3.5$ TeV. For other values of M_{WR} it scales as M_{WR}^{-4}.

If both light and heavy neutrino exchange contribute, the half-lives are given by

$$[\tau_{1/2}^{0\nu}]^{-1} = G_{0\nu}^{(0)} \left| M_{0\nu} \frac{\langle m_\nu \rangle}{m_e} + M_{0\nu_h} \eta \right|^2 . \qquad (27)$$

It is interesting to note here the possibility of interference between light and heavy neutrino exchange, as emphasised recently by several authors. The limits presented in Figs. 9, 10,11 are based on the calculation with M-S SRC. If CCM SRC are used, they should be multiplied by ~ 1.2 (light neutrino exchange) and ~ 2.0 (heavy neutrino exchange).

III. $2\nu\beta\beta$ DECAY

A. Matrix elements

As mentioned in the previous Sect. II, the calculated matrix elements of the GT operator in single-β decay appear to be systematically larger than those extracted from the measured ft values of allowed GT transitions. To take into account these results, it has been found convenient to "renormalize" the value of g_A to be used in a particular model calculation by introducing an effective

Table XIV. Left: Calculated half-lives for neutrinoless double-β decay with exchange of heavy neutrinos for $\eta = 2.75 \times 10^{-7}$ and $g_A = 1.269$. Right: Upper limits of $|\eta|$ and lower limits of heavy neutrino mass (see text for details) from current experimental limit from a compilation of Barabash [58]. The value reported by Klapdor-Kleingrothaus *et al.* [59], IGEX collaboration [60], and the recent limit from KamLAND-Zen [61] and EXO [62] are also included.

Decay	$\tau^{0\nu_h}_{1/2}(10^{24}\text{yr})$	$\tau^{0\nu_h}_{1/2,exp}(\text{yr})$	$\lvert\eta\rvert(10^{-6})$	$\langle m_{\nu_h}\rangle(\text{GeV})$
^{48}Ca$\rightarrow^{48}$Ti	0.77	$> 5.8 \times 10^{22}$	$<$1.00	$>$0.26
^{76}Ge$\rightarrow^{76}$Se	0.95	$> 1.9 \times 10^{25}$	$<$0.061	$>$4.2
		1.2×10^{25} [a]	0.077	3.362
		$> 1.6 \times 10^{25}$ [b]	$<$0.066	$>$3.88
^{82}Se$\rightarrow^{82}$Kr	0.40	$> 3.6 \times 10^{23}$	$<$0.29	$>$0.89
^{96}Zr$\rightarrow^{96}$Mo	0.07	$> 9.2 \times 10^{21}$	$<$0.77	$>$0.34
^{100}Mo$\rightarrow^{100}$Ru	0.03	$> 1.1 \times 10^{24}$	$<$0.0047	$>$5.5
^{110}Pd$\rightarrow^{110}$Cd	0.12			
^{116}Cd$\rightarrow^{116}$Sn	0.07	$> 1.7 \times 10^{23}$	$<$0.17	$>$1.5
^{124}Sn$\rightarrow^{124}$Te	0.39			
^{128}Te$\rightarrow^{128}$Xe	3.71	$> 1.5 \times 10^{24}$	$<$0.43	$>$0.60
^{130}Te$\rightarrow^{130}$Xe	0.19	$> 2.8 \times 10^{24}$	$<$0.071	$>$3.6
^{136}Xe$\rightarrow^{136}$Ba	0.29	$> 5.7 \times 10^{24}$ [c]	$<$0.061	$>$4.2
		$> 1.6 \times 10^{25}$ [d]	$<$0.116	$>$2.2
^{148}Nd$\rightarrow^{148}$Sm	0.14			
^{150}Nd$\rightarrow^{150}$Sm	0.02	$> 1.8 \times 10^{22}$	$<$0.27	$>$0.96
^{154}Sm$\rightarrow^{154}$Gd	0.38			
^{160}Gd$\rightarrow^{160}$Dy	0.06			
^{198}Pt$\rightarrow^{198}$Hg	0.18			

[a] Ref. [59]
[b] Ref. [60]
[c] Ref. [61]
[d] Ref. [62]

$g_{A,eff,\beta}$ defined as

$$\left(\frac{g_{A,eff,\beta}}{g_A}\right) = \frac{|M_{exp,\beta}|}{|M_{th,\beta}|}, \tag{28}$$

where $g_A = 1.269$ and M_β are the matrix elements for single-β decay. The ratio $(g_{A,eff}/g_A)$ is also called quenching, q, or hindrance, $h = 1/q$, factor. The quenching of g_A comes from two effects: (i) the limited model space in which the calculation is done and (ii) the contribution of non-nucleonic degrees of freedom, Δ,.... The first type of quenching depends strongly on the size of the model space used in the calculation and is thus model dependent. It was extensively investigated in light nuclei, $A \sim 20$, in the 1970's [65–67] within the framework of ISM where it was found that $g_{A,eff} \cong 1.0$, $q \cong 0.75$. In heavy nuclei, of particular interest in this paper, the question of quenching was first discussed by Fujita and Ikeda [68] in 1965. These authors analyzed β-decay in mass $A \sim 120$ nuclei within the framework of various models (pairing, pairing plus quadrupole, etc.) and found very small quenching factors, $q \simeq 0.2-0.3$ thus stimulating the statement that "massive" renormalization of g_A occurs in heavy nuclei [67]. The second type of quenching was extensively investigated theoretically in the 1970's [69–71]. This effect does not depend much on the nuclear model used in the calculation, but rather on the mechanism of coupling to non-nucleonic degrees of freedom. It is being re-investigated currently within the framework of chiral field theory (EFT) [72] and there are hints that it has a complex structure, in particular that it may depend on momentum transfer and that it may lead in some cases to an enhancement rather than a quenching.

The values of $g_{A,eff}$ depend crucially on the model used through the size and composition of the model space, especially on whether or not spin-orbit partners are included in the calculation. For example, while QRPA includes spin-orbit partners, IBM-2 and ISM do not. Conversely, in ISM calculations the size of the model space is $\sim 10^9$, while in QRPA and IBM-2 it is much smaller. In order to extract $g_{A,eff,\beta}$ for a given mass number A, one needs to do a calculation of single-β decay in that region and compare with experiment where available. Within the context of IBM-2, some calculations were done in the 1980's [73]. Very recently, the problem has been readdressed and results will be published soon [74].

Double-β decay depends on g_A as g_A^4 and thus its quenching is of extreme importance. Since $2\nu\beta\beta$ decay has now been measured in several nuclei, it provides another way to estimate $g_{A,eff}$ which we denote by $g_{A,eff,2\nu\beta\beta}$. In this section, we attempt an estimation of $g^{\text{IBM}-2}_{A,eff,2\nu\beta\beta}$ within the framework of IBM-2 in the closure approximation and also extract $g^{\text{ISM}}_{A,eff,2\nu\beta\beta}$ within the framework of ISM in the non-closure approximation.

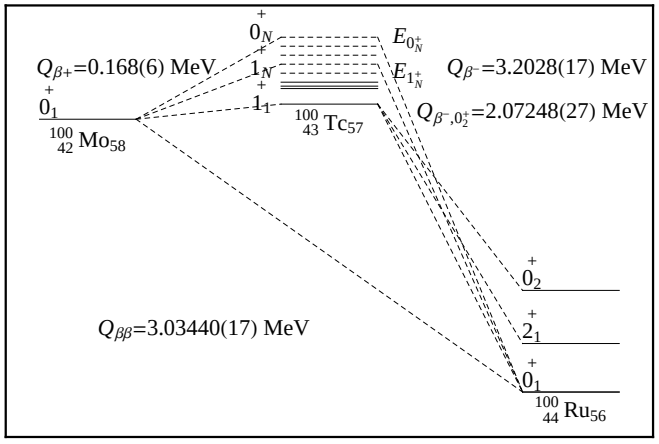

Figure 12. The decay $^{100}_{42}\mathrm{Mo}_{58} \rightarrow ^{100}_{44}\mathrm{Ru}_{56}$ is shown as an example of $2\nu\beta\beta$ decay.

The extraction of $g^{\mathrm{IBM-2}}_{A,eff,2\nu\beta\beta}$ in the non-closure approximation will be presented in the forthcoming publication mentioned above [74].

$2\nu\beta\beta$ is a process allowed by the standard model and thus in principle exactly calculable. The theory of $2\nu\beta\beta$ decay was developed by Primakoff and Rosen [19], Konopinski [76], Doi *et al.* [1] and Haxton *et al.* [21]. The calculation of $2\nu\beta\beta$ turns out to be more complex than that of $0\nu\beta\beta$.

(i) The closure approximation may not be good and one needs to evaluate explicitly the matrix elements to and from the individual 1^+_N and 0^+_N states in the intermediate odd-odd nucleus, Fig. 12,

$$M^{(2\nu)}_{GT,N} = \frac{\left\langle 0^+_F \left\| \tau^\dagger \vec{\sigma} \right\| 1^+_N \right\rangle \left\langle 1^+_N \left\| \tau^\dagger \vec{\sigma} \right\| 0^+_I \right\rangle}{\frac{1}{2}\left(Q_{\beta\beta} + 2m_e c^2\right) + E_{1^+_N} - E_I}, \tag{29}$$

and

$$M^{(2\nu)}_{F,N} = \frac{\left\langle 0^+_F \left\| \tau^\dagger \right\| 0^+_N \right\rangle \left\langle 0^+_N \left\| \tau^\dagger \right\| 0^+_I \right\rangle}{\frac{1}{2}\left(Q_{\beta\beta} + 2m_e c^2\right) + E_{0^+_N} - E_I}. \tag{30}$$

This evaluation has been done in selected nuclei within the framework of pnQRPA [77], the proton-neutron microscopic anharmonic vibrator approach (pnMAVA) [78, 79], and ISM [38, 80, 81] and it has been programmed very recently within the framework of the proton-neutron interacting boson-fermion model (IBFM-2) [74]. The calculation requires the difficult task of determining the structure of the intermediate odd-odd nucleus.

(ii) The phase space factors (PSF) cannot be exactly separated from the nuclear matrix elements. These factors must be calculated separately for each state 1^+_N and 0^+_N. In order to calculate half-lives and other observable quantities the product of the PSF factors $G^{(i)}_{2\nu,N}$ and matrix elements must be calculated and the contributions summed over all individual states. This is a daunting problem compounded by the fact that in most calculations the giant Gamow-Teller resonance that contributes to the matrix elements is not included in the model space.

The separation of PSF and nuclear matrix elements can be done in two cases: (1) The closure approximation (CA) and (2) the single-state dominance (SSD) approximation [82–86]. In both cases, the inverse half-life can be written as

$$\left[\tau^{2\nu}_{1/2}\right]^{-1} = G^{(0)}_{2\nu} \left| m_e c^2 M_{2\nu} \right|^2. \tag{31}$$

In the closure approximation (CA), the matrix elements $M_{2\nu}$ can be written as

$$\begin{aligned} M_{2\nu} &= g_A^2 M^{(2\nu)}, \\ M^{(2\nu)} &= -\left[\frac{M^{(2\nu)}_{GT}}{\tilde{A}_{GT}} - \left(\frac{g_V}{g_A}\right)^2 \frac{M^{(2\nu)}_F}{\tilde{A}_F}\right], \end{aligned} \tag{32}$$

where

$$\begin{aligned} M^{(2\nu)}_{GT} &= \left\langle 0^+_F \left| \sum_{nn'} \tau^\dagger_n \tau^\dagger_{n'} \vec{\sigma}_n \cdot \vec{\sigma}_{n'} \right| 0^+_I \right\rangle, \\ M^{(2\nu)}_F &= \left\langle 0^+_F \left| \sum_{nn'} \tau^\dagger_n \tau^\dagger_{n'} \right| 0^+_I \right\rangle. \end{aligned} \tag{33}$$

The closure energies $\tilde{A}_{GT}$ and $\tilde{A}_F$ are defined by

$$\begin{aligned} \tilde{A}_{GT} &= \frac{1}{2}\left(Q_{\beta\beta} + 2m_e c^2\right) + \left\langle E_{1^+,N} \right\rangle - E_I, \\ \tilde{A}_F &= \frac{1}{2}\left(Q_{\beta\beta} + 2m_e c^2\right) + \left\langle E_{0^+,N} \right\rangle - E_I, \end{aligned} \tag{34}$$

where $\langle E_N \rangle$ is a suitable chosen excitation energy in the intermediate odd-odd nucleus. The Fermi matrix elements are suppressed by isospin considerations and are often neglected. In case they are not, care must be taken since the closure energy $\tilde{A}_F$ is different from the closure energy $\tilde{A}_{GT}$, although, for simplicity $\tilde{A}_{GT} = \tilde{A}_F = \tilde{A}$ is often used.

In the single state dominance (SSD) approximation, the matrix elements are given by

$$\begin{aligned} M^{(2\nu)}_{GT,SSD} &= \frac{\left\langle 0^+_F \left\| \tau^\dagger \vec{\sigma} \right\| 1^+_1 \right\rangle \left\langle 1^+_1 \left\| \tau^\dagger \vec{\sigma} \right\| 0^+_I \right\rangle}{\frac{1}{2}\left(Q_{\beta\beta} + 2m_e c^2\right) + E_{1^+_1} - E_I}, \\ M^{(2\nu)}_{F,SSD} &= \frac{\left\langle 0^+_F \left\| \tau^\dagger \right\| 0^+_1 \right\rangle \left\langle 0^+_1 \left\| \tau^\dagger \right\| 0^+_I \right\rangle}{\frac{1}{2}\left(Q_{\beta\beta} + 2m_e c^2\right) + E_{0^+_1} - E_I}, \end{aligned} \tag{35}$$

where $E_{1^+_1}$ and $E_{0^+_1}$ are the energies in the intermediate odd-odd nucleus of the single state that dominates the decay. From these one can form the quantities

$$\begin{aligned} M^{(2\nu)}_{SSD} &= -\left[M^{(2\nu)}_{GT,SSD} - \left(\frac{g_V}{g_A}\right)^2 M^{(2\nu)}_{F,SSD}\right], \\ M_{2\nu,SSD} &= g_A^2 M^{(2\nu)}_{SSD}, \end{aligned} \tag{36}$$

and calculate the half-lives from (25), with $G^{(0)}_{2\nu}$ given by $G^{(0)}_{2\nu,SSD}$.

B. Results

In this article, we present results of a calculation of the nuclear matrix elements for $2\nu\beta\beta$ in the closure approximation (CA) using the transition operator of Sect. II. A. In this case only the terms $\tilde{h}^F_{VV}$ and $\tilde{h}^{GT}_{AA}$ are considered. An advantage of the closure approximation for $2\nu\beta\beta$ decay is that the nuclear matrix elements can be calculated using the same method discussed in Sect. II, by simply replacing the neutrino potential $v(p)$ by

$$v_{2\nu}(p) = \frac{\delta(p)}{p^2}, \tag{37}$$

which is the Fourier-Bessel transform of the configuration space potential $V(r) = 1$. Since our purpose here is a direct comparison of $2\nu\beta\beta$ and $0\nu\beta\beta$ decays, this avoids possible systematic and accidental errors. The closure approximation (CA) is not expected to be good for $2\nu\beta\beta$ decay, since only 1^+ and 0^+ intermediate states in the odd-odd nucleus contribute to the decay. We use it here only as an *estimate*, with appropriately chosen closure energy [2, p.71] in order to extract $g_{A,eff,2\nu\beta\beta} \equiv g_{A,eff}$ which is the purpose of this section.

Our calculated matrix elements for $2\nu\beta\beta$ decay are shown in Table XV. Also here as in Table III we have separated the class of nuclei where protons and neutrons occupy the same major shell from those where they do not, and added $A = 48$ at the bottom of the table. The problem of spuriosity of the Fermi matrix elements is here even more acute than in the case of $0\nu\beta\beta$. In the absence of isospin violation, all Fermi matrix elements for $2\nu\beta\beta$ should be exactly zero. Breaking of isospin is present in all calculations (ISM, QRPA, IBM-2, DFT, HFB). Within the model space and in the closure approximation that we are using, we have a large breaking for nuclei in which protons and neutrons occupy the same major shell and zero breaking in the others. The small value ~ 0.02 in Table XV is an indication of our numerical accuracy in calculating overlap of wave functions. From the dimensionless matrix elements in Table XV and the values of $\tilde{A}$ we calculate the values of $|m_e c^2 M^{(2\nu)}|$ given in Table XVI. In constructing this table we have taken into account only the GT matrix elements, since as mentioned above, the IBM-2 F matrix elements are largely spurious in nuclei where protons and neutrons occupy the same major shell.

We investigate two choices of $\tilde{A}_{GT}$. The first choice is that taken from Ref. [21] or estimated by the systematics, $\tilde{A}_{GT} = 1.12A^{1/2}$ MeV, where A without tilde denotes the mass number. In cases where transitions between spin-orbit partners dominate, one expects the single state dominance (SSD) to be appropriate. Our second choice is SSD for $_{40}$Zr, $_{42}$Mo, $_{46}$Pd, and $_{48}$Cd, where the dominant transition is $g_{9/2}$-$g_{7/2}$, and $_{60}$Nd where the dominant transition is $h_{11/2}$-$h_{9/2}$. In the same table we also show the values of the matrix elements in the ISM without the closure approximation [38]. The ISM calculation

Table XV. $2\nu\beta\beta$ matrix elements (dimensionless) to the ground state (columns 2 and 3) and to the first excited state (columns 4 and 5) using the microscopic interacting boson model (IBM-2) in the closure approximation.

	0^+_1		0^+_2	
A	$M^{(2\nu)}_{GT}$	$M^{(2\nu)}_{F}$	$M^{(2\nu)}_{F}$	$M^{(2\nu)}_{GT}$
76	4.34	-2.69	-1.35	1.99
82	3.50	-2.39	-0.83	1.03
96	2.22	0.02	0.00	0.04
100	2.94	0.03	0.00	0.39
110	2.98	0.03	0.01	1.48
116	2.31	0.02	0.01	0.86
124	2.80	-1.60	-1.34	2.15
128	3.63	-1.99	-1.53	2.65
130	3.31	-1.79	-1.45	2.59
136	2.76	-1.44	-0.83	1.63
148	1.24	0.02	0.00	0.17
150	1.54	0.02	0.00	0.29
154	1.91	0.02	-0.00	0.05
160	2.99	0.02	0.01	0.51
198	1.00	0.01	0.00	0.03
48	1.57	-1.08	-4.77	5.02

are all in nuclei in which protons and neutrons occupy the same major shell. By comparing these calculations with those in IBM-2 with the Fermi matrix elements set to zero we see that the two calculations have the same behavior with mass number but differ by a factor of approximately 2. The last columns in Table XVI gives the values of the matrix elements $|M^{eff}_{2\nu}|$ extracted from experiment [8].

If we write the matrix elements $M_{2\nu}$ as

$$M^{eff}_{2\nu} = \left(\frac{g_{A,eff}}{g_A}\right)^2 M_{2\nu}, \tag{38}$$

where $(g_{A,eff}/g_A) = q$ is a quenching factor, by comparing the experimental values $M_{2\nu,exp}$ with the calculated values (or the experimental half-lives with those calculated using PSF factors of [8]) we can extract the values of $g_{A,eff}$. These are given in Table XVII and Fig. 13 for IBM-2 (GT) and ISM. As mentioned in Sect. II, the renormalization of g_A to $g_{A,eff}$ is due to two main reasons: (1) Limitation of the model space in which calculations are done and (2) omission of non-nucleonic degrees of freedom (Δ, N^*, ...). As a result, one expects $g_{A,eff}$ to have a smooth behavior with A to which shell effects are superimposed. We see from Fig. 13 that this is approximately the case if we assume SSD in $_{40}$Zr, $_{42}$Mo, $_{48}$Cd, and $_{60}$Nd. This is consistent with previous analyses [85, 86]. The smooth behavior can be parametrized as $g^{\rm IBM-2}_{A,eff} = 1.269A^{-\gamma}$, with $\gamma = 0.18$ for IBM-2 (GT). This gives for the neutron (A=1) the free value. The same

Table XVI. Calculated values of $2\nu\beta\beta$ matrix elements in IBM-2 with $g_A = 1.269$ and ISM with $g_A = 1.25$.

	$\tilde{A}(MeV)$		$\left\|m_e c^2 M^{(2\nu)}\right\|$				
A	$\tilde{A}^{CA}_{GT}$	$\tilde{A}^{SSD}_{GT}$	IBM-2 $\overset{CA}{GT}$	IBM-2 $\overset{SSD}{GT}$	ISM[a]	exp[b] $\overset{CA}{exp}$	exp[b] $\overset{SSD}{exp}$
48	7.72[c]		0.10		0.05	0.038(3)	
76	9.41[c]		0.24		0.15	0.118(5)	
82	10.1[c]		0.18		0.15	0.083(4)	
96	11.0	2.20	0.10	0.51		0.080(4)	0.075(4)
100	11.2	1.69	0.13	0.89		0.206(7)	0.185(6)
110	11.8	1.89	0.13	0.80			
116	12.1	1.88	0.10	0.63		0.114(5)	0.106(4)
124	12.5		0.12				
128	12.5[c]		0.15			0.044(6)	
130	13.3[c]		0.13		0.07	0.031(4)	
136	13.1		0.11		0.06	0.0182(17)	
148	13.6		0.05				
150	13.7	1.88	0.06	0.42		0.058(4)	0.052(4)
154	13.9		0.07				
160	14.2		0.11				
198	15.8		0.03				

[a] Ref. [38]
[b] Ref. [8]
[c] Ref. [21]

Table XVII. Value of $g_{A,eff}$ extracted from experiment.

Nucleus	$\tau_{1/2,\mathrm{exp}}(10^{18}$ yr)[a] exp	$\tau_{1/2}(10^{18}$ yr) IBM-2 $\overset{CA}{GT}$	$\tau_{1/2}(10^{18}$ yr) IBM-2 $\overset{SSD}{GT}$	$g_{A,eff}$ IBM-2 $\overset{CA}{GT}$	$g_{A,eff}$ IBM-2 $\overset{SSD}{GT}$	$g_{A,eff}$ ISM
^{48}Ca	44^{+6}_{-5}	2.30		0.61(2)		0.90(3)
^{76}Ge	1500 ± 100	144		0.71(1)		0.90(2)
^{82}Se	92 ± 7	7.68		0.68(1)		0.74(2)
^{96}Zr	23 ± 2	5.31	0.187	0.88(2)	0.38(1)	
^{100}Mo	7.1 ± 0.4	6.46	0.117	1.24(2)	0.46(1)	
^{116}Cd	28 ± 2	14.5	0.306	1.08(2)	0.41(1)	
^{128}Te	1900000 ± 400000	65600	1170	0.55(3)		
^{130}Te	680^{+120}_{-110}	15.5		0.49(2)		0.67(3)
^{136}Xe	2110 ± 250[b]	23.0		0.41(2)		0.57(2)
^{150}Nd	8.2 ± 0.9	3.21	0.048	1.00(3)	0.35(1)	

[a] Ref. [87]
[b] Ref. [88]

type of analysis can be done for the ISM. The values of $g_{A,eff}$ extracted by comparing the calculated and experimental matrix elements are also shown in Table XVII and Fig. 13. We see that $g_{A,eff}$ in ISM has the same behavior as in IBM-2, except for larger value. It can be parametrized as $g^{\mathrm{ISM}}_{A,eff} = 1.269A^{-\gamma}$ with $\gamma = 0.12$. In Ref. [38] the value 0.93 was used for ^{48}Ca, ^{76}Ge and ^{82}Se and 0.71 for ^{130}Te and ^{136}Xe.

The question of how to extract $g_{A,eff}$ in QRPA has been the subject of many investigations [11]. In this case $g_{A,eff}$ can be extracted either from $2\nu\beta\beta$ or from single-β decay [89]. We do not discuss this extraction here but simply note that the values extracted are similar but larger than those in Table XVII and Fig. 13.

Values of $(g_{A,eff})^2$ can also be extracted from single-β decay or EC using a Fermi-surface quasi-particle model (FSQP) [90] where

$$(g_{A,eff})^2 = g_i^{eff} g_f^{eff} \tag{39}$$

is the product of g_i^{eff} for the transition from even-even to odd-odd and g_f^{eff} for the transition from odd-odd to even-even. The values obtained in this way [91] are also similar to those in Table XVII and Fig. 13. Finally, very recently, values of $g^{\mathrm{IBM-2}}_{A,eff,2\nu\beta\beta}$ have been extracted from a $2\nu\beta\beta$ calculation without the closure approximation for ^{128,130}Te$\rightarrow^{128,130}$Xe decay with similar results [74]. As one can see from the discussion in the

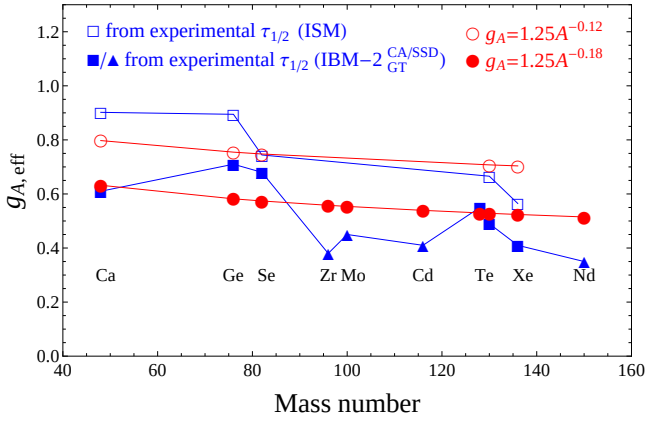

Figure 13. (Color online) Value of $g_{A,eff}$ extracted from experiment for IBM-2 and ISM.

paragraphs above, the extraction of the actual value of $g_{A,eff}$ is highly dependent on the model calculations and the assumptions made. All extractions, however, indicate values of $g_{A,eff}$in the range $g^{\rm ISM}_{A,eff} \sim 0.57 - 0.90$ $g^{\rm IBM-2}_{A,eff} \sim 0.35 - 0.71$ depending on mass number A and on SSD or CA approximation, with decreasing trend with A.

It is of considerable interest to analyze the impact that the quenching of g_A to $g_{A,eff}$ observed in single-β and $2\nu\beta\beta$ decay may have on $0\nu\beta\beta$. The question of whether or not the quenching of g_A is the same in $2\nu\beta\beta$ as in $0\nu\beta\beta$ is the subject of debate, since only the states 1^+ and 0^+ in the intermediate odd-odd nucleus contribute to $2\nu\beta\beta$, while all multipoles contribute to $0\nu\beta\beta$. Two lines of thought have been considered : (1) Only GT (1^+) is quenched and other multipoles are not. (2) All multipoles are equally quenched. The experimental information on higher multipoles is meager, with only some hints coming from muon capture. The contribution of different intermediate states $J^\pm$ to $0\nu\beta\beta$ decay in ^{100}Mo was investigated in Ref. [13] within the framework of QRPA-Tü. It was found that the contribution of 1^+ is sizeable, of opposite sign than that of the other multipoles and very much parameter (g_{pp}) dependent. In view of this sizeable contribution, even if the other multipoles are not quenched, there is going to be an effect coming from the 1^+ multipole.

In order to investigate the possible impact of quenching of g_A, we present in Table XVIII, the predicted half-lives under assumption of "maximal quenching" in which all multipoles are quenched with

$$g^{\rm IBM-2}_{A,eff} = 1.269A^{-0.18}, \qquad g^{\rm ISM}_{A,eff} = 1.269A^{-0.12}. \tag{40}$$

In the same table we show for comparison the unquenched values with $g_A = 1.269$ discussed in Sect. II, and shown in Table XIII. We observe that while the ISM unquenched values are a factor of approximately 2 smaller than IBM-2, the quenched values of both calculations are similar, since the smaller calculated matrix elements in ISM are compensated in part by a larger value of $g_{A,eff}$. (This statement is not correct in ^{48}Ca where the simple parametrization $1.269A^{-\gamma}$ fails.) It appears therefore that the difference of a factor of 2 in the calculated nuclear matrix elements in IBM-2 and ISM is simply due to the difference in the size of the model space and thus in the renormalization of g_A.

Another important question in this context is whether or not g_V is quenched. From conserved vector current (CVC) we expect g_V not to be quenched, at least as far as the contribution of $(\Delta, N^*, ...)$ is concerned. On the other side, the size of the model space certainly affects the Fermi matrix elements, through the overlap of the initial and final wave functions and their isospin purity. Thus, if one defines

$$\left(\frac{g_{V,eff,\beta}}{g_V}\right) = \frac{|M_{exp,\beta}|}{|M_{th,\beta}|}, \tag{41}$$

where $g_V = 1$, one may reasonably expect a quenching of the Fermi matrix elements as well. Whether or not the quenching factor for $g_{V,eff,\beta}$ is the same as for $g_{A,eff,\beta}$ is not clear. We are currently investigating this question with the context of IBM-2. Within this model, it appears also that the question of isospin violation can be dealt with by means of a quenching of the Fermi matrix elements. The question of how to project into states of good isospin was investigated years ago by introducing the concept of F-spin (isospin of the pairs) [35, p.134]. Because of the complexity of the problem, we do not discuss it here but defer it to a subsequent publication. In the columns "maximally quenched" in Table XVIII we have assumed equal quenching both for g_V and g_A and thus no quenching in the ratio g_V/g_A. This assumption introduces an additional error of about 10% in the quenched calculation.

In conclusion, Table XVIII gives ranges of expected half-lives based on IBM-2 and ISM calculations for unquenched, $g_A = 1.269$, $g_V = 1$, and "maximally quenched" values of $g_{A,eff}$, $g_{V,eff}$. The actual situation may in fact be in between these two extreme values. Similar analyses have been done within QRPA except that a quenched value $g_{A,eff} = 1.0$ is used while $g_{V,eff} = 1$ is unquenched [13].

IV. CONCLUSIONS

In this article we have presented a consistent evaluation of nuclear matrix elements in $0\nu\beta\beta$, $0\nu_h\beta\beta$, Sect. II, and $2\nu\beta\beta$ decay, Sect. III, within the framework of IBM-2 in the closure approximation. All calculations can be done simultaneously by replacing the neutrino "potential" $v(p)$ as summarized in Appendix A. While the closure approximation is expected to be good for $0\nu\beta\beta$ and

Table XVIII. Predicted half-lives in $0\nu\beta\beta$ decay with unquenched and maximally quenched g_A, $g_{A,eff}^{\rm IBM-2}$ and $g_{A,eff}^{\rm ISM}$ obtained from $2\nu\beta\beta$ decay.

	$\tau_{1/2}^{0\nu}(10^{24}\text{yr})$			
	IBM-2		ISM	
Decay	unquenched	maximally quenched	unquenched	maximally quenched
^{48}Ca→^{48}Ti	1.03	16.8	13.9	89.2
^{76}Ge→^{76}Se	1.45	32.8	8.65	69.1
^{82}Se→^{82}Kr	0.52	12.4	2.22	18.5
^{96}Zr→^{96}Mo	0.77	20.5		
^{100}Mo→^{100}Ru	0.46	12.5		
^{110}Pd→^{110}Cd	1.60	47.1		
^{116}Cd→^{116}Sn	0.78	24.0		
^{124}Sn→^{124}Te	0.91	29.2	2.73	27.6
^{128}Te→^{128}Xe	8.53	281	33.5	344.4
^{130}Te→^{130}Xe	0.44	14.5	1.70	17.6
^{136}Xe→^{136}Ba	0.62	21.5	2.39	25.3
^{148}Nd→^{148}Sm	2.54	97.4		
^{150}Nd→^{150}Sm	0.30	11.0		
^{154}Sm→^{154}Gd	5.34	201		
^{160}Gd→^{160}Dy	0.80	31.0		
^{198}Pt→^{198}Hg	3.77	170		

$0\nu_h\beta\beta$ decay since the virtual neutrino momentum is of order 100 MeV/c and thus much larger than the scale of nuclear excitations, it is not expected to be good for $2\nu\beta\beta$ decay where the neutrino momentum is of order of few MeV/c and thus of the same scale of nuclear excitation. Furthermore, for $2\nu\beta\beta$, the single state dominance (SSD) may be a better approximation. Hence the $2\nu\beta\beta$ calculation in Sect. III should viewed only as an estimate.

By using the $0\nu\beta\beta$ matrix elements and phase space factors of Ref. [8], we have calculated the expected $0\nu\beta\beta$ half-lives in all nuclei of interest with $g_A = 1.269$ and $g_V = 1$, given in Table XIII and Fig. 9. This is the main result of this paper, and should be compared with other calculations, QRPA, ISM, DFT, HFB, with the same (or similar) values of $g_A = 1.25 - 1.269$ and $g_V = 1$.

Finally, in Sect. III, we have examined the impact that a quenching of g_A may have on $0\nu\beta\beta$ decay and reported in Table XVIII results of a quenched calculation with the quenching factor extracted from $2\nu\beta\beta$ decay. This calculation is speculative since we have no experimental information to confirm whether or not quenching is the same for all multipoles in the intermediate nucleus. Our assessment is that, while in the unquenched case the situation is such that current (GERDA, CUORE) and planned experiments may reach accuracies to detect at least the inverted hierarchy of Fig. 10, in the quenched case only the degenerate case can be detected in the foreseeable future. The results presented here point to the necessity of further studies and refinements, the crucial ones being: (i) An improved treatment of the Fermi matrix elements, (ii) an improved treatment of SRC, and (iii) the determination of the quenching factors $g_{A,eff}$ for all multipoles in $0\nu\beta\beta$ decay. The latter is of importance not only for IBM-2 but also for all other model calculations.

V. ACKNOWLEDGEMENTS

This work was supported in part by U.S.D.O.E. Grant DE-FG-02-91ER-40608 and Fondecyt Grant No. 1120462. We wish to thank all the experimental groups that have stimulated our work, in particular A. Bettini, S.E. Elliott, E. Fiorini, G. Gratta, A. McDonald, S. Schoenert and K. Zuber.

VI. APPENDIX A: NEUTRINO POTENTIALS AND THEIR RADIAL INTEGRALS

The neutrino potentials used in this article are given in Table XIX. The function $H(r)$ is the Fourier-Bessel transform of $2\pi^{-1}[p(p+\tilde{A})]^{-1}$, and is given in [2], Appendix 2, and in Eq. (19) of [3]. It does not have an explicit form. We note, however that, when the closure energy $\tilde{A}$ goes to zero, then $v(p) = 2\pi^{-1}p^{-2}$, and its Fourier-Bessel transform becomes the Coulomb potential, $H(r) \to 1/r$. The neutrino potential is a long-range potential, since the mass of the exchanged particle is very small. The situation is opposite in the case of heavy neutrino exchange. In this case, the mass of the exchanged particle is very large and thus the potential is a contact interaction $\delta(r)/r^2$. For $2\nu\beta\beta$ decay, the potential does not have a radial dependence and thus it is a contact interaction in momentum space. The values of $\tilde{A}$ used in this article are given in Table XVI. The radial integrals of the neutrino potential are best calculated in momentum space using the Horie method [92] as

discussed in the Appendix A of [15], with harmonic oscillator single-particle wave functions with oscillator parameter $\nu = M\omega/\hbar$, where M is the nucleon mass. In this article, we take $\nu = \nu_0 A^{-1/3}$, where A is the mass number and $\nu_0 = 0.994$ fm^{-2}.

Table XIX. Neutrino potentials used in this article.

Transition	$V(r)$	$v(p)$
$0\nu\beta\beta$	$H(r)$	$\frac{2}{\pi}\frac{1}{p(p+\bar{A})}$
$0\nu_h\beta\beta$	$\frac{1}{m_e m_p}\frac{\delta(r)}{r^2}$	$\frac{2}{\pi}\frac{1}{m_e m_p}$
$2\nu\beta\beta$	1	$\frac{\delta(p)}{p^2}$

VII. APPENDIX B: SINGLE PARTICLE ENERGIES AND STRENGTH OF INTERACTION

In order to calculate the pair structure constants we need the single-particle and -hole energies and strength of interaction. We give in Tables XX-XXII, the single-particle and -hole energies used in this article. We generate the pair structure constants by diagonalizing the surface delta interaction (SDI) in the two identical particle states, pp, nn. The strength of the (isovector) interaction, A_1, is also given in Tables XX-XXII. It is obtained by fitting the 2^+-0^+ energy difference in nuclei with either two proton (proton holes) or two neutron (neutron holes). For ^{48}Ca$\rightarrow$ ^{48}Ti decay, we need also the strength of the interaction in the $1f_{7/2}$ shell, given by $A_1 = 0.510$ MeV. The calculation of the pair structure constants can be improved by a better choice of the interaction and of the single-particle energies. We have tried different choices of the single-particle energies and included the variation of the corresponding radial integrals in the estimate of the sensitivity to parameter changes.

Table XX. SDI strength values A_1 and single particle and hole energies (in MeV) in the $N, Z = 28 - 50$ shell. The energies are taken from the spectra of ^{57}Cu for proton particles, from isotones $N = 50$ for proton holes and from the spectra of ^{57}Ni for neutron holes.

Orbital	Protons (particles) $A_1 = 0.366$	Protons (holes) $A_1 = 0.264$	Neutrons (holes) $A_1 = 0.280$
$2p_{1/2}$	1.106	0.931	1.896
$2p_{3/2}$	0.000	2.198	3.009
$1f_{5/2}$	1.028	2.684	2.240
$1g_{9/2}$	3.009	0.000	0.000

Table XXI. SDI strength values A_1 and single particle and hole energies (in MeV) in the $N, Z = 50 - 82$ shell. The energies are taken from the spectra of ^{133}Sb for protons particles, from the spectra of ^{207}Tl for proton holes, from the spectra of ^{91}Zr for neutron particles, from the spectra of ^{131}Sn for neutron holes.

Orbital	Protons (particles) $A_1 = 0.221$	Protons (holes) $A_1 = 0.200$	Neutrons (particles) $A_1 = 0.269$	Neutrons (holes) $A_1 = 0.163$
$3s_{1/2}$	2.990	0.000	1.205	0.332
$2d_{3/2}$	2.690	0.350	2.042	0.000
$2d_{5/2}$	0.960	1.670	0.000	1.655
$1g_{7/2}$	0.000	2.700	2.200	2.434
$1h_{11/2}$	2.760	1.340	2.170	0.070

Table XXII. SDI strength values A_1 and single particle energies (in MeV) in the $N = 82 - 126$ shell. The energies are taken from [93] for neutron particles and from the spectra of ^{208}Pb for neutron holes.

Orbital	Neutrons (I) (particles) A_1 =0.147	Neutrons (holes) A_1 =0.150
$3p_{1/2}$	2.250	0.000
$3p_{3/2}$	1.500	0.900
$2f_{5/2}$	2.600	0.570
$2f_{7/2}$	0.000	2.340
$1h_{9/2}$	2.450	3.410
$1i_{13/2}$	2.800	1.630

VIII. APPENDIX C: PARAMETERS OF THE IBM-2 HAMILTONIAN

A detailed description of the IBM-2 Hamiltonian is given in [27] and [94]. For most nuclei, the Hamiltonian parameters are taken from the literature [95–107]. The quality of the description can be seen from these references and ranges from very good to excellent (see Fig. 4). The only nuclei for which we have done new calculations are ^{48}Ti, ^{96}Zr, ^{124}Sn, ^{136}Xe , ^{160}Gd, and ^{160}Dy. The new calculations are done using the program NPBOS [94] adapted by J. Kotila. They include energies, B(E2) values, quadrupole moments, B(M1) values, magnetic moments, etc. The calculations for ^{160}Gd and ^{160}Dy have just been published [108]. A paper with those for ^{48}Ti is in preparation [109]. The quality of these, as well as of the unpublished results for ^{96}Zr is equal to that of the results obtained previously [95–107]. For the semi-magic nuclei $^{116-124}$Sn and ^{136}Xe, we have obtained the parameters by a fit to the energy of the low lying states using the same procedure as Ref. [103] for ^{116}Sn, while ^{48}Ca has been taken as doubly magic. This procedure is compatible with the Generalized Seniority (GS) scheme, that appears to be good for semi-magic nuclei as extensively discussed in the 1980's for pairing plus quadrupole interactions, and as shown recently for realistic interactions [110].

Table XXIII. Hamiltonian parameters employed in the IBM-2 calculation of the final wave functions along with their references.

Nucleus	ϵ_{d_ν}	ϵ_{d_π}	κ	χ_ν	χ_π	ξ_1	ξ_2	ξ_3	$c_\nu^{(0)}$	$c_\nu^{(2)}$	$c_\nu^{(4)}$	$c_\pi^{(0)}$	$c_\pi^{(2)}$	$c_\pi^{(4)}$	$\omega_{\nu\nu}$	$\omega_{\pi\pi}$	$\omega_{\nu\pi}$	w_ν	y_ν
^{48}Ti[a]	1.11	1.11	-0.20	-0.30	-0.70	1.00	1.00	1.00											
^{76}Ge [95]	1.20	1.20	-0.21	1.00	-1.20	-0.05	0.10	-0.05											
^{76}Se [96]	0.96	0.96	-0.16	0.50	-0.90			-0.10											
^{82}Se [96]	1.00	1.00	-0.28	1.14	-0.90			-0.10											
^{82}Kr [97]	1.15	1.15	-0.19	0.93	-1.13	-0.10		-0.10											
^{96}Zr[a]	1.00	1.00	-0.20	-2.20	0.65										0.17	0.17	0.33		
^{96}Mo [98]	0.73	1.10	-0.09	-1.20	0.40	-0.10	0.10	-0.10	-0.50	0.10									
^{100}Mo [98]	0.55	1.00	-0.06	-1.20	0.40	-0.10	0.10	-0.10	-0.60	0.20	0.10								
^{100}Ru [99]	0.89	0.89	-0.18	-1.00	0.40				0.60	0.09	-0.13								
^{110}Pd [100]	0.78	0.60	-0.13	0.00	-0.30	0.20	0.04	0.00	-0.26	-0.29	-0.30	-0.26	-0.29	-0.03					
^{110}Cd [101]	0.92	0.92	-0.15	-1.10	-0.80	1.10	0.109	1.10	0.07	-0.17	0.16								
^{116}Cd [102]	0.85	0.85	-0.27	-0.58	0.00	-0.18	0.24	-0.18	-0.15	-0.06									
^{116}Sn [103]	1.32								-0.50	-0.22	-0.07							-0.06	0.04
^{124}Sn[b]	1.10								-0.30	-0.16	-0.20							0.30	0.02
^{124}Te [102]	0.82	0.82	-0.15	0.00	-1.20	-0.18	0.24	-0.18	0.10										
^{128}Te [102]	0.93	0.93	-0.17	0.50	-1.20	-0.18	0.24	-0.18	0.30	0.22									
^{128}Xe [104]	0.70	0.70	-0.17	0.33	-0.80	-0.18	0.24	-0.18	0.30										
^{130}Te [102]	1.05	1.05	-0.20	0.90	-1.20	-0.18	0.24	-0.18	0.30	0.22									
^{130}Xe [104]	0.76	0.76	-0.19	0.50	-0.80	-0.18	0.24	-0.18	0.30	0.22									
^{136}Xe[b]		1.31										-0.04	0.01	-0.02					
^{136}Ba [104]	1.03	1.03	-0.23	1.00	-0.90	-0.18	0.24	-0.18	0.30	0.10									
^{148}Nd [105]	0.70	0.70	-0.10	-0.80	-1.20	-0.12	0.24	0.90				0.40	0.20						
^{148}Sm [105]	0.95	0.95	-0.12	0.00	-1.30	-0.12	0.24	0.90					0.05						
^{150}Nd [105]	0.47	0.47	-0.07	-1.00	-1.20	-0.12	0.24	0.90				0.40	0.20						
^{150}Sm [105]	0.70	0.70	-0.08	-0.80	-1.30	-0.12	0.24	0.90					0.05						
^{154}Sm [105]	0.43	0.43	-0.08	-1.10	-1.30	-0.12	0.24	0.90					0.05						
^{154}Gd [105]	0.55	0.55	-0.08	-1.00	-1.00	-0.12	0.24	0.90				-0.20	-0.10						
^{160}Gd [108]	0.42	0.42	-0.05	-0.80	-1.00	0.08	0.08	0.08				-0.20	-0.10						
^{160}Dy [108]	0.44	0.44	-0.06	-0.80	-0.90	0.08	0.08	0.08				-0.05	-0.15						
^{198}Pt [106]	0.58	0.58	-0.18	1.05	-0.80	-0.10	0.08	-0.10	0.00	0.02	0.00								
^{198}Hg [107]	0.55	0.55	-0.21	1.00	-0.40		0.08		0.37	0.25	0.16								

[a] Parameters fitted to reproduce the spectroscopic data of the low lying energy states.
[b] GS parameters fitted to reproduce the spectroscopic data of the low lying energy states.

[1] M. Doi *et al.*, Prog. Theor. Phys. **66**, 1739 (1981); M. Doi *et al.*, Prog. Theor. Phys. **69**, 602 (1983).
[2] T. Tomoda, Rep. Prog. Phys. **54**, 53 (1991).
[3] F. Šimkovic, G. Pantis, J.D. Vergados, and A. Faessler, Phys. Rev. C **60**, 055502 (1999).
[4] Y. Fukuda *et al.*, Phys. Rev. Lett. **81**, 1562 (1998).
[5] Q.R. Ahmad *et al.*, Phys. Rev. Lett. **89**, 011301 (2002).
[6] K. Eguchi *et al.*, Phys. Rev. Lett. **90**, 021802 (2003).
[7] V. Tello, M. Nemevšek, F. Nesti, G. Senjanović, and F. Vissani, Phys. Rev. Lett. **106**, 151801 (2011).
[8] J. Kotila and F. Iachello, Phys. Rev. C **85**, 034316 (2012).
[9] J. Kotila and F. Iachello, in preparation.
[10] J. Barea, J. Kotila, and F. Iachello, in preparation.
[11] J. Suhonen and O. Civitarese, Phys. Rep. **300**, 123 (1998).
[12] A. Faessler and F. Šimkovic, J. Phys. G: Nucl. Part. Phys **24**, 2139 (1998).
[13] F. Šimkovic, A. Faessler, V. Rodin, P. Vogel, and J. Engel, Phys. Rev. C **77**, 045503 (2008).
[14] E. Caurier, J. Menéndez, F. Nowacki, and A. Poves, Phys. Rev. Lett. **100**, 052503 (2008).
[15] J. Barea and F. Iachello, Phys. Rev. C **79**, 044301 (2009).
[16] F. Iachello and J. Barea, Nucl. Phys. B (Proc. Suppl.) **217**, 5 (2011).
[17] F. Iachello, J. Barea, and J. Kotila, *Proc. of the Int. Workshop MEDEX11*, AIP Conf. Proc. **1417**, 62 (2011).
[18] W.H. Furry, Phys. Rev. **56**, 1184 (1939).
[19] H. Primakoff and S.P. Rosen, Rep. Prog. Phys. **22**, 121 (1959).
[20] A. Molina and P. Pascual, Nuovo Cimento A **41**, 756 (1977).
[21] W. C. Haxton and G. J. Stephenson Jr., Prog. Part. Nuc. Phys. **12**, 409 (1984).
[22] O. Dumbrajs *et al.*, Nucl. Phys. B **216**, 277 (1983).
[23] M. R. Schindler and S. Scherer, Eur. Phys. J. A **32**, 429 (2007).
[24] W.-M. Yao *et al.*, J. Phys. G **33**, 1 (2006).

[25] G. A. Miller and J. E. Spencer, Ann. Phys. (NY) **100**, 562 (1976).
[26] F. Šimkovic, A. Faessler, H. Müther, V. Rodin, and M. Stauf, Phys. Rev. C **79**, 055501 (2009).
[27] A. Arima, T. Otsuka, F. Iachello and I. Talmi, Phys. Lett. B **66**, 205 (1977).
[28] T. Otsuka, A. Arima and F. Iachello, Nucl. Phys. A **309**, 1 (1978).
[29] J. P. Elliott and A. P. White, Phys. Lett. B **97**, 169 (1980).
[30] J. P. Elliott and J. A. Evans, Phys. Lett. B **101**, 216 (1981).
[31] P. D. Duval and B. R. Barrett, Nucl. Phys. A **376**, 213 (1982).
[32] F. Šimkovic, M. Nowak, W. A. Kamiński, A. A. Raduta, and A. Faessler, Phys. Rev. C **64**, 035501 (2001).
[33] J. Menéndez, A. Poves, E. Caurier, and F. Nowacki, Nucl. Phys. A **818**, 139 (2009).
[34] V.A. Rodin, A. Faessler, F. Šimkovic, and P. Vogel, Erratum Nucl. Phys. A **793**, 213 (2007).
[35] F. Iachello and A. Arima, *The Interacting Boson Model* (Cambridge University Press, Cambridge, 1987).
[36] J. Suhonen, *Proc. of Beauty in Physics: Theory and Experiment*, AIP Conf. Proc. **1488**, 326 (2012), and references therein.
[37] J. Suhonen, private communication.
[38] E. Caurier, F. Nowacki, and A. Poves, Int. J. Mod. Phys. E **16**, 552 (2007).
[39] J. Suhonen, J. Phys. G: Nucl. Part. Phys. **19**, 139 (1993).
[40] D.-L. Fang, A. Faessler, V. Rodin, and F. Šimkovic, Phys. Rev. C **82**, 051301 (R) (2010).
[41] D.-L. Fang, A. Faessler, V. Rodin, and F. Šimkovic, Phys. Rev. C **83**, 034320 (2011).
[42] K. Chaturvedi, R. Chandra, P.K. Rath, P.K. Raina, and J.G. Hirsch, Phys. Rev. C **78**, 054302 (2008).
[43] T.R. Rodríguez and G. Martínez-Pinedo, Phys. Rev. Lett. **105**, 252503 (2010).
[44] T.R. Rodríguez, private communication.
[45] E. Lisi, *Proc. of the Int. Workshop MEDEX11*, AIP Conf. Proc. **1417**, 74 (2011).
[46] J. Suhonen and O. Civitarese, Phys. Lett. B **668**, 277 (2008).
[47] J. P. Schiffer *et al.*, Phys. Rev. Lett. **100**, 112501 (2008).
[48] B. P. Kay *et al.*, Phys. Rev. C **79**, 021301(R) (2009).
[49] H. Feldmeier, T. Neff, R. Roth, and J. Schnack, Nucl. Phys. A **632**, 61 (1998).
[50] J.J. Gómez-Cadenas *et al.*, J. Cosm. Astropart. Phys. **6**, 007 (2011).
[51] A. Faessler, S. Kovalenko, F. Šimkovic, and J. Schwieger, Phys. Rev. Lett. **78**, 183 (1997).
[52] G. Prézeau, M. Ramsey-Musolf, and P. Vogel, Phys. Rev. D **68**, 034016 (2003).
[53] A. Faessler, G. L. Fogli, E. Lisi, A. M. Rotunno, and F. Šimkovic, Phys. Rev. D **83**, 113015 (2011).
[54] J. Suhonen, *From Nucleons to Nuclei: Concepts of Microscopic Nuclear Theory* (Springer Verlag, Berlin, 2007).
[55] J. Toivanen and J. Suhonen, Phys. Rev. Lett. **75**, 410 (1995).
[56] M. Kortelainen and J. Suhonen, Phys. Rev. C **75**, 051303(R) (2007).
[57] F. Boehm and P. Vogel, *Physics of Massive Neutrinos* (Cambridge University Press, New York, 1992).
[58] A.S. Barabash, Phys. Atom. Nucl. **74**, 603 (2011).
[59] H.V. Klapdor-Kleingrothaus *et al.*, Phys. Lett. B **586**, 198 (2004).
[60] C. E. Aalseth *et al.* (IGEX collaboration), Phys. Rev. D **65**, 092007 (2002).
[61] A. Gando *et al.* (KamLAND-Zen collaboration), Phys. Rev. C **85**, 045504 (2012).
[62] M. Auger *et al.* (EXO collaboration) Phys. Rev. Lett. **109**, 032505 (2012).
[63] C. Arnaboldi *et al.* (CUORICINO collaboration), Phys. Rev. C **78**, 035502 (2008),
[64] R. Arnold, *et al.* (NEMO collaboration), Nucl. Phys. A **765**, 483 (2006).
[65] D. H. Wilkinson, Phys. Rev. C **7**, 930 (1973).
[66] D. H. Wilkinson, Nucl. Phys. A **209**, 470 (1973).
[67] D. H. Wilkinson, Nucl. Phys. A **225**, 365 (1974).
[68] J. Fujita and K. Ikeda, Nucl. Phys. **67**, 145 (1965).
[69] M. Ericson, Ann. Phys. **63**, 562 (1971).
[70] S. Barshay, G. E. Brown, and M. Rho, Phys. Rev. Lett. **32**, 787 (1974).
[71] A. Arima, M. Ichimura and K. Shimizu, J. Phys. Soc. Jpn. Suppl. **34**, 526 (1973).
[72] J. Menéndez, D. Gazit, and A. Schwenk, Phys. Rev. Lett. **107**, 062501 (2011).
[73] F. Dellagiacoma, and F. Iachello, Phys. Lett. B **218**, 399 (1989).
[74] N. Yoshida and F. Iachello, to be submitted to Prog. Theor. Phys. (2012).
[75] G. L. Fogli *et al.*, Phys. Rev. D **75**, 053001 (2007); D **78**, 033010 (2008).
[76] E.J. Konopinski, *Theory of Beta Radioactivity* (Oxford University Press, Oxford, 1966).
[77] J. Suhonen, Phys. Atom. Nucl. **61**, 1286 (1998); J. Suhonen, Phys. Atom. Nucl. **65**, 2176 (2002).
[78] J. Kotila, J. Suhonen, and D. S. Delion, J. Phys. G: Nucl. Part. Phys. **36**, 045106 (2009).
[79] J. Kotila, J. Suhonen, and D. S. Delion, J. Phys. G: Nucl. Part. Phys. **37**, 015101 (2010).
[80] E. Caurier, F. Nowacki, A. Poves, and J. Retamosa, Phys. Rev. Lett. **77**, 1954 (1996).
[81] M. Horoi, S. Stoica,and B. A. Brown, Phys. Rev. C **75**, 034303 (2007).
[82] J. Abad, A. Morales, R. Nuñez-Lagos, and A.F. Pacheco, An. Fis. A **80**, 9 (1984); J. Phys. (Paris) 45, 147 (1984).
[83] A. Griffiths and P. Vogel, Phys. Rev. C **46**, 181 (1992).
[84] O. Civitarese and J. Suhonen, Phys. Rev. C **58**, 1535 (1998).
[85] F. Šimkovic, P. Domin, and S.V. Semenov, J. Phys. G: Nucl. Part. Phys. **27**, 2233 (2001).
[86] P. Domin, S. Kovalenko, F. Šimkovic, and S.V. Semenov, Nucl. Phys. A **753**, 337 (2005).
[87] A.S. Barabash, Phys. Rev. C **81**, 035501(2010).
[88] N. Ackerman *et al.* (EXO Collaboration), Phys. Rev. Lett. **107**, 212501 (2011).
[89] J. Suhonen, Phys. Lett. B **607**, 87 (2005).
[90] H. Ejiri, J. Phys. Soc. Japan **78**, 074201 (2009).
[91] H. Ejiri, Part. Nucl. Phys. **64**, 249 (2010).
[92] H. Horie and K. Sasaki, Prog. Theor. Phys. **25**, 475 (1961).
[93] S. Pittel, P. D. Duval, and B.R. Barrett, Ann. Phys. **144**, 168 (1982).
[94] T. Otsuka and N. Yoshida, User's Manual of the program NPBOS, Report No. JAERI-M 85-094, 1985.

[95] P. D. Duval, D. Goutte, and M. Vergnes, Phys. Lett. B **124**, 297 (1983).
[96] U. Kaup, C. Mönkemeyer, and P. V. Brentano, Z. Physik A **310**, 129 (1983).
[97] U. Kaup and A. Gelberg, Z. Physik A **293**, 311 (1979).
[98] H. Dejbakhsh, D. Latypov, G. Ajupova, and S. Shlomo, Phys. Rev. C **46**, 2326 (1992).
[99] P. Van Isacker and G. Puddu, Nucl. Phys. A **348**, 125 (1980).
[100] K. H. Kim, A. Gelberg, T. Mizusaki, T. Otsuka, and P. Von Brentano, Nucl. Phys. A **604**, 163 (1996).
[101] A. Giannatiempo, A. Nannini, A. Perego, P. Sona, and G. Maino, Phys. Rev. C **44**, 1508 (1991).
[102] M. Sambataro, Nucl. Phys. A **380**, 365 (1982).
[103] S. Cacciamani, G. Bonsignori, F. Iachello, and D. Vretenar, Phys. Rev. C **53**, 1618 (1996).
[104] G. Puddu, O. Scholten, and T. Otsuka, Nucl. Phys. A **348**, 109 (1980).
[105] O. Scholten, Ph. D. thesis, University of Groningen, The Netherlands (1980).
[106] R. Bijker, A. E. L. Dieperink, and O. Scholten, Nucl. Phys. A **344**, 207 (1980).
[107] A. F. Barfield, B. R. Barrett, K. A. Sage, and P. D. Duval, Z. Physik A **311**, 205 (1983).
[108] J. Kotila, K. Nomura, L. Guo, N. Shimizu, and T. Otsuka, Phys. Rev. C **85**, 054309 (2012), and private communication.
[109] J. Kotila, S. Lenzi *et al.*, in preparation.
[110] M. A. Caprio, F. Q. Luo, K. Cai, Ch. Constantinou, and V. Hellemans, J. Phys. G: Nucl. Part. Phys **39**, 105108 (2012).